# Nested Autonomy:
# A Robust Operational Paradigm for Distributed Ocean Sensing

**Henrik Schmidt**
**Michael R. Benjamin**
**Stephanie Petillo**
**Toby Schneider**
**Raymond Lum**
**Laboratory for Autonomous Marine Sensing Systems**
**Massachusetts Institute of Technology**
**http://lamss.mit.edu**

## Abstract

Ocean monitoring and observation is undergoing a dramatic paradigm shift from platform-centric, human-controlled sensing, processing and interpretation, toward distributed sensing concepts using networks of autonomous underwater vehicles. Being dependent on acoustic communication with a channel capacity many orders of magnitude smaller than the air and land-based equivalents, the operation of such new distributed undersea observation systems require a much higher level of autonomous, distributed data processing and control than land- and air-based equivalents. This chapter describes a new command and control paradigm, *Nested Autonomy*, inherently suited for the layered communication infrastructure provided by the low-bandwidth underwater acoustic communication and the intermittent RF connectivity. Implemented using the open-source MOOS-IvP behavior-based, autonomous command and control architecture, it provides the fully integrated sensing, modeling and control that allows each platform to autonomously detect, classify, localize and track an episodic event in the ocean, without depending on any operator command and control. The prosecution of an event, such as the detection and tracking of a sub-sea volcanic plume or an oceanographic feature, may be initiated by the operators or entirely autonomously by an onboard detection capability. The event information collected by each node in the network is reported back to the operators by transmitting an event report, using a dedicated command and control language. Collaborative processing and control is exploited when the communication channel allows, e.g. collaborative tracking of a coastal front, or the tracking of manmade sources or marine mammals.

## 1. Introduction: Nested Autonomy for Ocean Observation Systems

The primary motivation for designing a distributed command and control architecture for undersea monitoring and observation is to achieve the ability to deploy a fleet of autonomous mobile marine platforms over a wide area of the ocean environment and over a long period of time with little or no human supervision. Concerns over effective coverage, communication range and safe operation of the platforms are all primary motivations of an effective form of autonomous control. The long duration of missions and unpredictable nature of the environment require the vehicles to adapt their missions and behave autonomously as events unfold. Conversely, practical concerns of marine operations over large areas require an element of

operator intervention over the course of time. These two characteristics can be at odds with each other in practice, but can be tempered by effective periodic communication through a network of fixed and mobile nodes co-deployed in a coordinated manner designed to balance individual platform and network objectives. The connectivity with and between the submerged assets of such networks is almost entirely dependent on underwater acoustic communication, except for rare and time-limited surfacings. Consequently, the undersea network nodes must operate with a communication infrastructure with severely limited bandwidth. Current underwater communication technology can robustly provide a point-to-point channel capacity in shallow water of less than a few hundred byte-km/minute, close to ten orders of magnitude smaller than modern electromagnetic communication protocols used for land- and air-based distributed, net-centric systems. Equally critical is the high latency and short communication windows inherently associated with communication between the human operator and the submerged assets, more severe than that experienced in interplanetary space exploration. Operational constraints for some applications prohibit the existence of permanent surface assets, which can provide a high-speed communication link with the operators. The connection of the operator to such systems is instead restricted to gateway vehicles, such as underwater gliders, which occasionally surface for a limited time and quickly relay short messages received acoustically from the submerged network nodes, and receive command and control commands which will subsequently be transmitted via the acoustic channel to the other nodes. The latencies using such a gateway vehicle on the continental shelf will typically be on the order of 10-60 minutes.

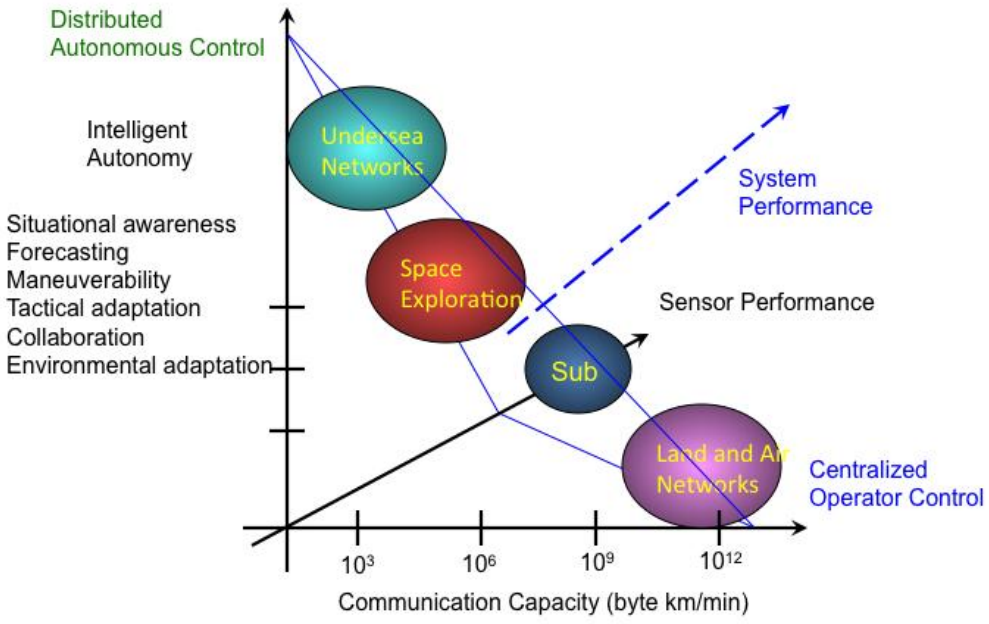


**Figure 1.** Performance trade-off between sensor performance, communication channel capacity and autonomy for net-centric sensing and observation systems

A typical acoustic or optical sensing system will generate data at a rate on the order of megabytes per second, for which the acoustic communication capacity of the undersea environment is totally inadequate for transmission of raw data back to the operators. Therefore, in contrast to the air and land-based equivalents, the data processing cannot be performed

centrally but must be largely distributed to the individual nodes. Similarly, real-time 'tethered' control of the underwater assets is made impossible by the latencies imposed by the use of occasionally surfacing gateway nodes. Consequently, real-time command and control decisions must be made locally on the nodes, in turn requiring that not only the data processing, but also the analysis and interpretation, traditionally performed by human operators, must be performed locally on the nodes. This requires fully integrated *sensing*, *modeling* and *control*, a significantly higher level of autonomy than required in most current applications of autonomous underwater vehicles (AUVs) - where the data collection and the control have been handled independently.

In addition to allowing for autonomous reaction to sensor input, the higher degree of autonomy enables the adaptive control of the mobile nodes to take optimal advantage of the environmental and tactical situation through modeling and forecasting. As illustrated in Fig. 1, such onboard intelligent autonomy may compensate for the reduction in performance associated with the limited sensing capabilities of small underwater vehicles and the limited undersea communication channel capacity and latency.

For ocean monitoring and observation systems, an important mission objective for the network is the detection, classification, and tracking of episodic - usually unpredictable - events. Such events include chemical plumes from undersea volcanoes or man-made systems, and biological phenomena such as algal blooms. Another important application of undersea sensing systems is the detection and tracking of marine mammals and man-made sources of sound in the presence of ambient noise. Without the possibility of transmitting large amounts of data back to the operators, the on-board autonomy must be capable of fully completing the mission objective of sampling and characterizing the event entirely autonomously, without any human intervention or assistance.

In addition to autonomously ***adapting*** to such episodic events, the individual nodes may take advantage of ***collaboration*** with other nodes, again without requiring the human operator in the loop (Benjamin, 2002). Thus, a cluster of network nodes within - at least occasional - acoustic communication range with each other may fuse its own data collected for the event with those obtained by and broadcast by other network nodes in the vicinity. For example, two AUVs with acoustic arrays may each track a marine mammal and collaboratively create an accurate localization solution by triangulation.

To enable effective and fully autonomous adaptation and collaboration for an undersea network with its inherently severe communication constraints, MIT has developed an operational ***Nested Autonomy*** architecture with fully integrated sensing, modeling and control within each autonomous underwater vehicle, clusters of assets, and the entire network (Schneider and Schmidt, 2010).

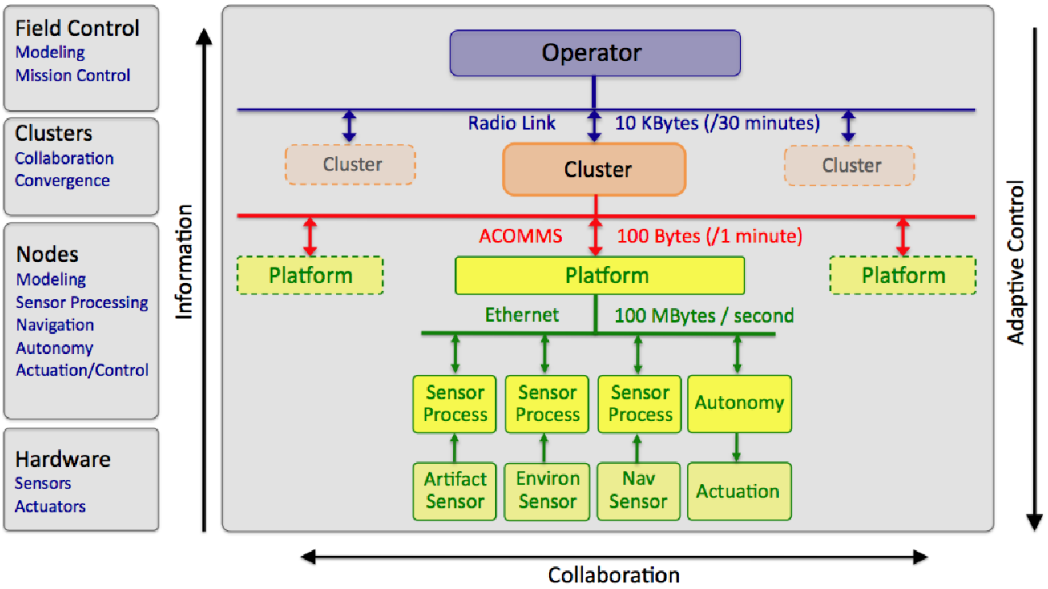


**Figure 2.** Nested Autonomy. The field operator is communicating with clusters of autonomous nodes through gateway assets occasionally surfacing for transmitting target reports and receiving network commands, e.g. through satellite radio communication, yielding high bandwidth, but latency of 10-60 minutes. The nodes in the cluster communicate acoustically at low bandwidth but low latency. The Node and Cluster Autonomy are designed accordingly.

The *Nested Autonomy* paradigm is exploiting the inherent layering of the communication infrastructure, illustrated in Fig. 2. The underwater network connectivity is being provided by low-bandwidth acoustic communication (ACOMMS), while the above-surface networking is handled by high-bandwidth, but latent, radio frequency (RF) communication through a regularly surfacing gateway node. On-board each node, the computer bus and Ethernet networking provides very high bandwidth communication between the sensing, modeling and control processes. The three layers of horizontal communication have vastly different bandwidths, ranging from 100 byte/min for the inter-node ACOMMS to 100 Mbyte/sec for the on-board systems. Equally important, the layers of the vertical connectivity differ significantly in latency and intermittency, ranging from virtually instantaneous connectivity of the on-board sensors and control processes to latencies of 10-60 minutes for information flowing to and from the field control (human) operators. As a result, adaptive control of the network assets with the operator in-the-loop is at best possible on an hourly basis, allowing the field operator to make tactical deployment decisions for the network assets based on, e.g., environmental forecasts and reports of interfering shipping lane distributions, etc. Shorter time scale adaptation, such as autonomously reacting to episodic environmental events or a node tracking a marine mammal acoustically must clearly be performed either at the *Node* level, or, if collaborative sensing is feasible, at the *Cluster* level.

The *Nested Autonomy* concept of operations (CONOPS) does not entirely eliminate the operator from the decision process. Thus, whenever a communication opportunity arises, the operational paradigm will take advantage of any information that can be received from the operator or collaborators in the cluster. On the other hand, the intermittency of the underwater acoustic communication channel makes it imperative that each node is capable of completing the mission objectives in the total absence of communication connectivity.

## 2. Concept of Operations (CONOPS)

### 2.1. Field-level

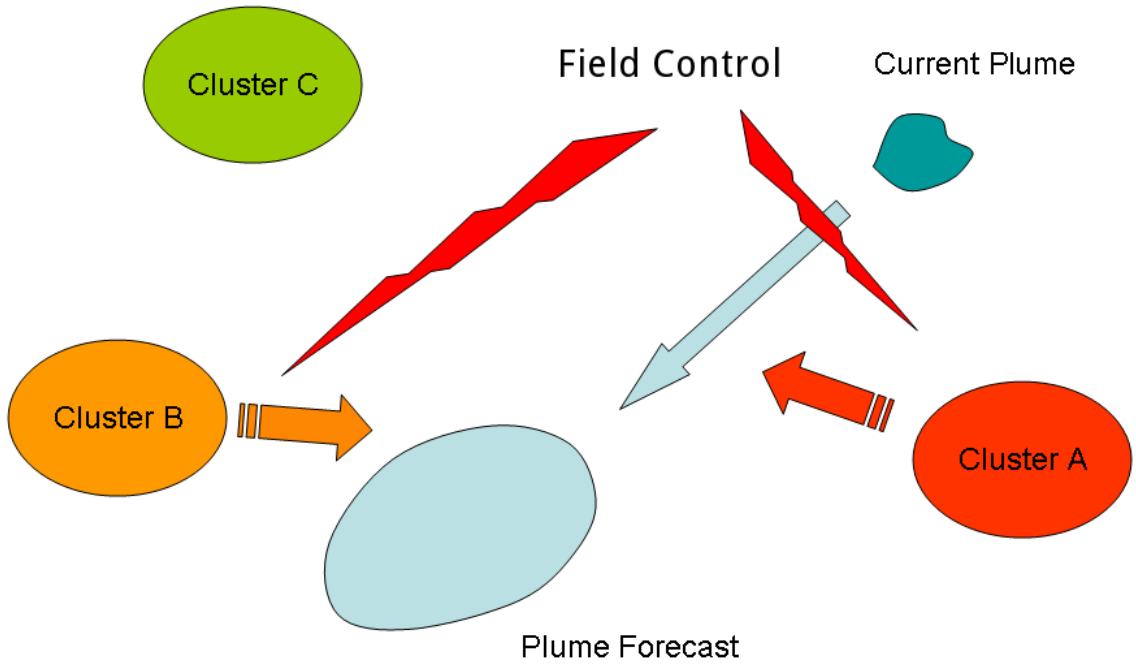


**Figure 3.** Field-level CONOPS. The Field Control is dispatching clusters to autonomously prosecute a chemical plume with a forecast path and expansion. Cluster A is instructed to initiate prosecution immediately since it is closest to the projected path. The 'downstream' Cluster B is alerted to be ready for action, while field control decides not to activate cluster C, which is not in the path of the plume.

The layered and clustered communication infrastructure illustrated in Fig. 2 naturally leads to a nested or layered concept of operations, which, as mentioned earlier, provides some optimal mixture of distributed autonomy and centralized control. Figure 3 shows a possible field-level concept of operations for an oceanographic observation system for capturing an episodic event, such as a chemical plume released by an undersea volcanic event. The target area is populated by a number of clusters, each with a number of mobile assets such as AUVs and gliders.

One of the adaptive responsibilities of the operators is to deploy the finite number of clusters in a pattern which is optimal for the current environmental situation and with the highest probability for capturing the episodic event of interest. The time scales for deployment and re-deployment are inherently long - on the order of hours to days - and is therefore highly dependent on reliable environmental and situational forecasts, often requiring a significant modeling and data assimilation infrastructure. Once deployed, it is assumed that each cluster is capable of autonomously Detecting, Classifying, Localizing and Tracking (DCLT) the episodic event of interest. This event *Prosecution* may be either cued by the operators through a surface communication gateway, or performed fully autonomously. Once a tracking solution and the nature of the event are determined, the result of the prosecution will be reported back to the

operators in the form of an *Event Report*. The human operators may then cue other clusters in the projected path of the event with whatever information is available, packaged into the format suitable for transmission through the Network, e.g. using the dynamic message coding scheme D-CCL (Schneider and Schmidt, 2012). The final crucial role of Field Control is the fusing of the *Event Reports* from the various clusters in the path of the event, gradually building up a more and more complete event track and description.

### 2.2. Cluster-level

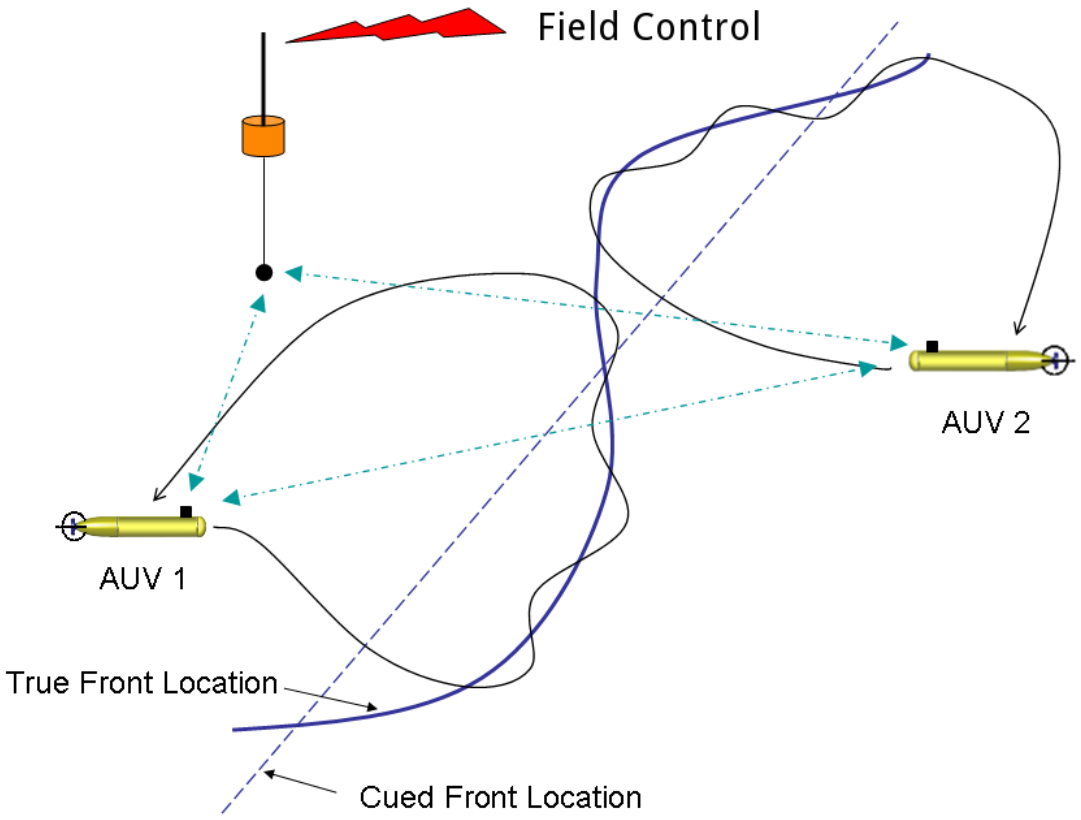


**Figure 4.** CONOPS for a cluster of AUV's with oceanographic sensors, and a gateway buoy for communication with Field Control. The position and heading of a front is cued to the vehicles via the gateway buoy and they initiate a Prosecute mission, autonomously detecting the front and subsequently mapping it by autonomously tracking the temperature gradient at the frontal boundary. The two AUVs coordinate the survey to increase coverage and avoid overlap.

Depending on the available assets, a wide spectrum of cluster compositions is conceivable, including gliders and propelled AUVs with chemical, biological and acoustic sensors. Figure 4 schematically shows how such cluster assets may be applied in response to an event cueing message from Field Control. The message identifies a front with a location and heading indicated

by the dashed line. After the message is received by a surface gateway buoy, it is broadcast using the acoustic modems. Nearby nodes, such as dormant, drifting or bottomed AUVs which pick up the message, will initiate a Prosecute behavior sequence - in this case the detection and subsequent mapping and tracking of a frontal boundary. Depending on the level of autonomy authorized by Field Control, the AUV may decide not to pursue the target event if there is little probability it will come within detection range.

If two or more nodes are prosecuting the event, each node may fuse the event information from the other nodes to produce a more accurate event characterization, and to optimize the coverage or resolution. Thus, in Fig. 4 the two vehicles coordinate their survey in order to not overlap and to increase coverage. Another example of collaborative control is a node which did not receive the original Prosecute command, but which, following the receipt of an Event Report from a prosecuting node, will determine whether the target event is likely to come within range, and then autonomously initiate a Prosecute sequence. All Event Reports generated by the prosecuting nodes are then collected by the communication gateway and transmitted back to Field Control via RF communication.

### 2.3 Node-level

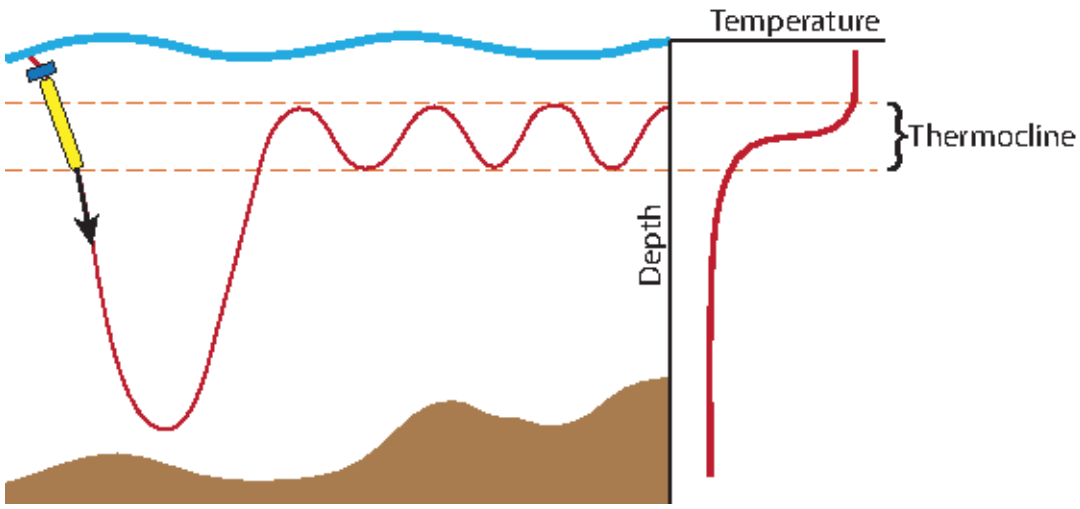


**Figure 5.** Concept of operations for an AUV detecting, classifying and tracking a coastal thermocline. Used with permission from (Petillo, Balasuriya, & Schmidt, 2010).

A suite of node-level CONOPS have been developed for both single node and collaborative detection and tracking of a variety of episodic events, such as the adaptive mapping of a front or a thermocline, and for tracking an acoustic source, such as a marine mammal or a man-made source of sound.

As an example, Fig. 5 shows the core adaptive Prosecute sequence developed for a propelled AUV for Detecting, Classifying, Localizing and Tracking (DCLT) a shallow water thermocline. The node CONOPS are described here for the tracking of a thermocline, but they can be directly mapped onto any other episodic event in the ocean environment, e.g. the tracking of a plume, where the collaborative, adaptive cluster autonomy is even more important by providing

simultaneously the resolution and coverage required for accurately localizing, classifying and tracking the event. Thus, the network must first detect and localize the plume, and then adaptively track its boundaries, a mission which obviously requires the vehicles to collaborate to cover the expanding spatial extent of the plume.

# 3. Autonomy

## 3.1 MOOS-IvP Autonomy Architecture and System

The core of the nested autonomy paradigm is MOOS-IvP (the Mission Oriented Operating Suite, with Interval Programming): the autonomous, integrated sensing, modeling and command and control framework on each individual platform. In combination with the collaborative cluster autonomy, the integrated node autonomy enables the adaptation which may compensate for the reduced physical sensor apertures of the unmanned underwater vehicles. The design of the autonomy system is based on three basic architectural components, extending the nesting into each individual sensor node:

- **Payload / Backseat Vehicle Architecture:** Low-level vehicle control is separated from the platform autonomy software, with the latter operating on a separate payload computer. This allows the same payload software and payload hardware to be integrated in vehicles of different size and different vehicle manufacturers.
- **Publish and Subscribe Software Application Architecture:** The payload software system is comprised of several distinct applications. The decision-making, sensor processing, communications handling, data logging, and many other applications are coordinated by the MOOS publish-subscribe middleware. The core MOOS middleware is lightweight, having no external dependencies and less than 1Mb compiled size. The 2012 release, MOOS V10, allows for improved high bandwidth and low latency communications, suitable for use on the Oxford autonomous car project. Hundreds of MOOS applications have been written for use on at least 20 different marine vehicle platform types. Applications are largely independent, defined only by their interface. Any application is easily replaceable with an improved version with a matching interface. Core MOOS and many common applications are publicly available along with source code under an Open Source LGPL license.
- **Behavior Based Decision Making Architecture:** The IvP Helm is a single MOOS application containing its own architecture of modular components - behaviors. The mission mode determines which behaviors are active, and competing behaviors are coordinated using multi-objective optimization using interval programming (Benjamin, Schmidt, Newman, & Leonard, 2010). Several common and powerful behaviors are available at www.moos-ivp.org, but users may augment this core capability with their own public or proprietary behaviors to suit new mission objectives.

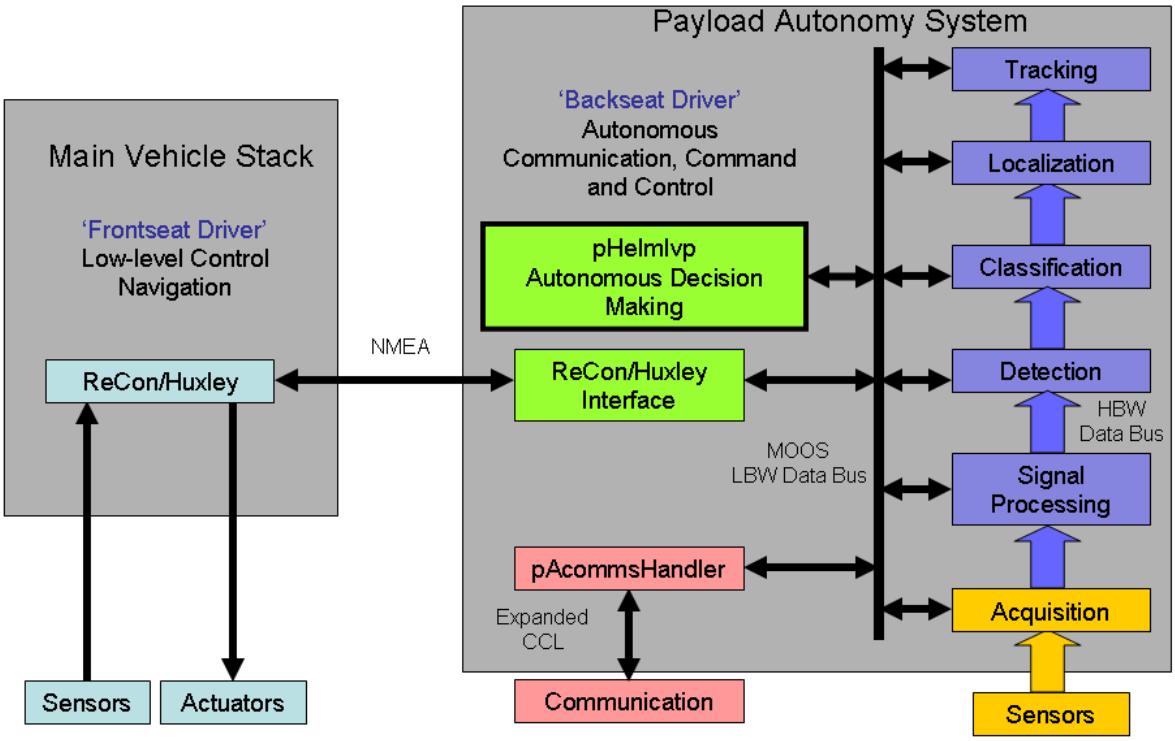


**Figure 6.** Schematic representation of the Payload Autonomy paradigm, where higher level adaptive control and network communication are handled by MOOS-IvP on the payload computer, while lower level control, navigation and vehicle safety are handled by the main vehicle computer using the native control software.

### 3.2 The Payload Autonomy Paradigm

To allow the MOOS-IvP network control to be applied on a variety of fixed and moving nodes with different control software, a *Payload Autonomy* paradigm was adopted and integrated with the MOOS-IvP control software infrastructure, and has subsequently been integrated into a wide variety of autonomous underwater vehicles and surface craft. This is achieved by adopting a hardware and software architecture that physically separates the sensing, communication, data processing, and associated adaptive autonomy from the basic platform control, illustrated schematically in Fig. 6. The idea is that all high-level control including the adaptation to measured and estimated parameters, is performed on a payload computer (PLC) running MOOS middleware, and including the IvP-Helm autonomous decision making engine. The payload will also handle all communication with the Network, either through a radio link while surfaced, or an acoustic modem when submerged. All lower level control, and basic navigation and platform safety tasks are handled by the native vehicle control software running on the main vehicle computer (MVC), for example *Huxley* on Bluefin vehicles and *Recon* on Remus vehicles. The communication between the PLC and the MVC is performed over a manufacturer-specific NMEA-type interface, operated by a dedicated MOOS process. The commands passed from the PLC to the MVC are simply continuous updates of desired heading, speed and depth, which the MVC then translates to desired rudder, thrust and elevator signals to the tail cone. The MVC will provide the PLC with a data stream containing all relevant navigation data. Thus, in a traditional

ship analogy, the PLC represents the bridge, the radio room and the sensing infrastructure, while the MVC represents the engine room and the navigation resources of the ship. In the same analogy, the Helm represents the "Captain," while the interface MOOS module represents the "Helmsman."

The MVC will also perform a series of basic safety tasks, including mission aborts due to bottom altitude limit violations, lack of commands from the PLC within a specified time, or an overall mission timeout. Higher level safety tasks such as exceeding the specified operational area, and individual behavior timeouts or failures, are handled by the PLC.

### 3.3 The MOOS-IvP Autonomy Architecture

The *Nested Autonomy* paradigm for distributed undersea sensing inherently involves reaction to situations and events that are deterministically unpredictable. Thus, the autonomy architecture cannot be based on the availability of a world model that can form the basis for the autonomous decision making. Instead, it requires a capability of fully autonomously adapting to the environmental and tactical situation associated with the phenomenon it is intended to measure. As such, it forms a clear example of the type of robotic system for which the Interval Programming (IvP) model for multi-objective behavior coordination was intended and developed. Thus, for example, an underwater vehicle tasked with detecting and tracking an acoustic source is faced with several, often conflicting objectives. It will likely have been assigned a station point, from which it should not move too far, while at the same time having to get close to the source to develop a reliable tracking solution. Also, depending on its sensing capability it may have a preferred heading for achieving tracking resolution. Also, if other vehicles in the vicinity are already tracking the target event, it may not be desirable for it to pursue the same source aggressively, but instead preserve power for future sensing tasks. MOOS-IvP provides exactly the flexibility and inherent multi-objective capability for implementing such high-level autonomy with adaptive and collaborative capabilities.

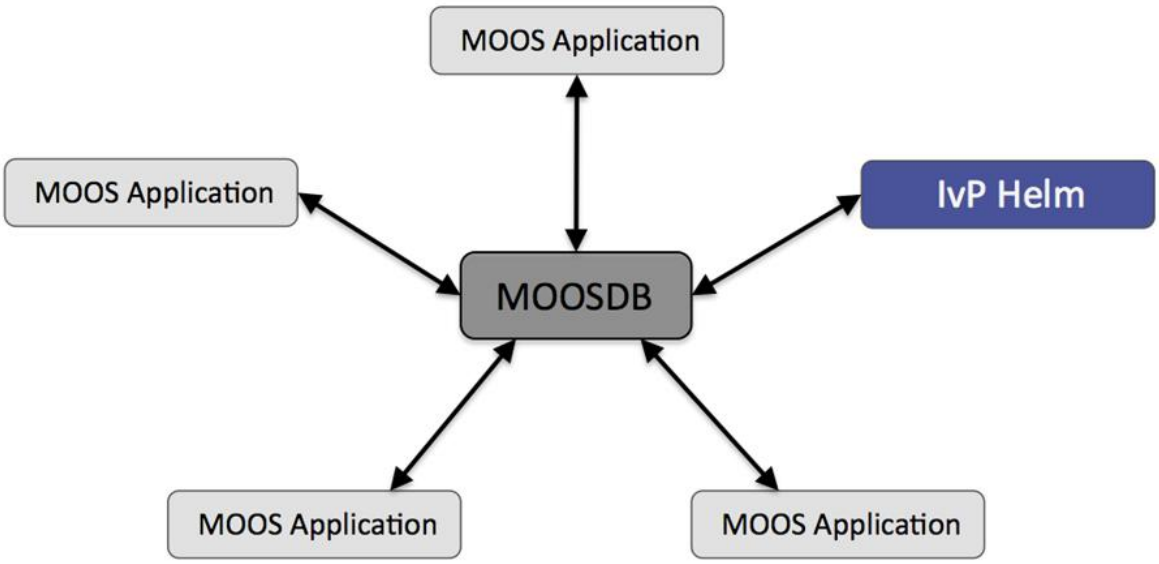

**Figure 7.** Modular software architecture based on the MOOS Middleware.

The MIT-LAMSS group's implementation of the *Nested Autonomy* concept of operations is using the MOOS middleware, supporting the modular 'star' software architecture illustrated in Fig. 7. As in all MOOS communities, the MOOS Database (MOOSDB) process is the core of the MOOS architecture and handles all communication between the processes (applications) using a publish-and-subscribe architecture. The various MOOS processes include all necessary control functions as well as sensing and processing modules, with the MOOSDB providing the unified interface standard that enables the fully autonomous integration of sensing, modeling,processing, and control. MOOS ensures a process executes its *Iterate* method at a specified frequency and handles new mail on each iteration in a publish-and-subscribe manner. The autonomy (IvP) helm runs as the MOOS process pHelmIvP.

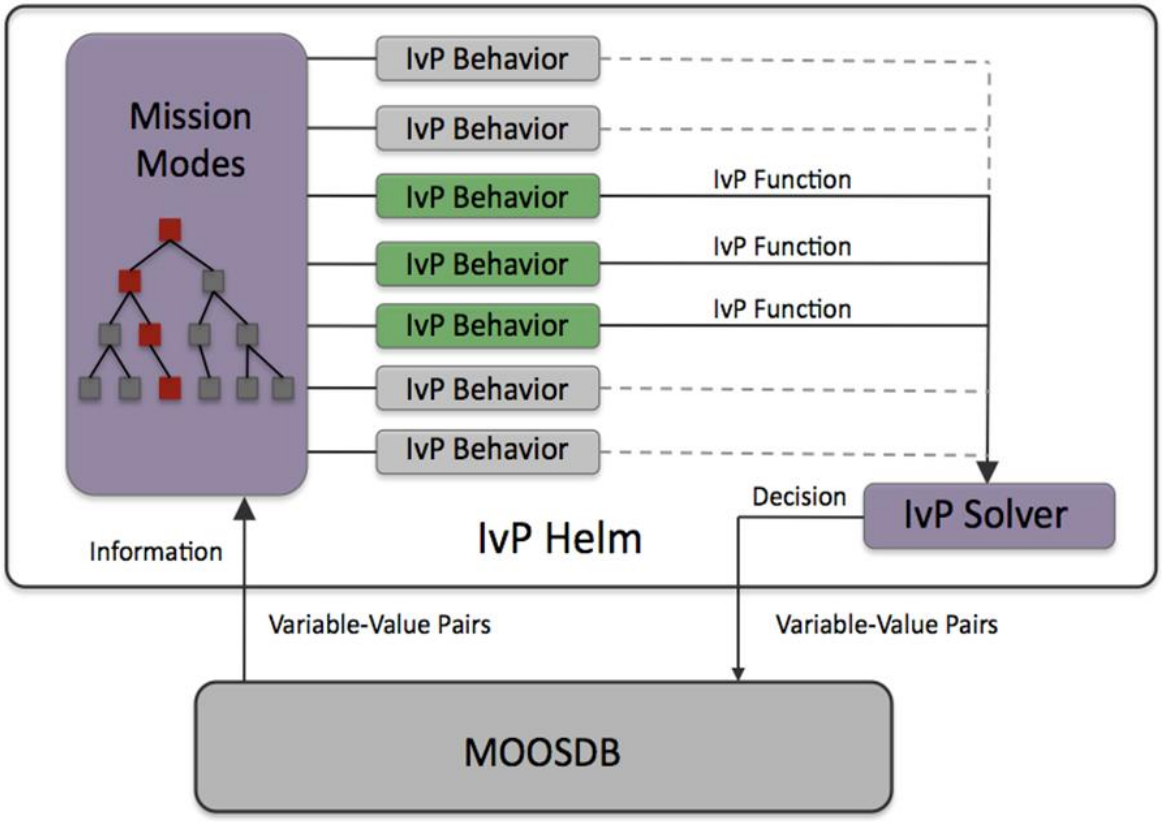


**Figure 8.** IvP-Helm autonomy architecture. The autonomy configuration defines a set of autonomy modes, each of which defines a set of active behaviors which provide objective functions for platform speed, heading and depth, which form the basis for the multi-objective optimization compromise provided to the platform by the IvP-Helm.

The fundamental architecture of the IvP-Helm autonomy configuration at the core of the Nested Autonomy paradigm is illustrated in Fig. 8. Because of the inherent latency and intermittency of the underwater communication environment, the mission-dependent autonomy configuration defines a finite set of autonomy *Modes* in which the autonomy will remain perpetually until specifically reassigned through a high level transition command, either from the topside command and control or an onboard mission control process. The autonomy mode structure is configured in a hierarchical tree structure, with the mode transitions achieved by a simple change in a MOOS control variable, thus requiring very limited communication from the operators. Note that this paradigm is in distinct contrast to traditional *scripted* autonomy, where mode transitions are in general predefined.

Another fundamental architectural principle illustrated in Fig. 8 is that each mode has a pre-configured set of *Behaviors*, each of which defines a set of objective functions for *Speed*, *Heading* and *Depth*, representing the utility of all allowed values for these variables. As in the case of the modes, the behaviors are perpetual, which means that they are running throughout the mission whenever the mode is active, although they may not contribute an objective function unless certain conditions are met. For example the vehicles will continuously run a collision avoidance behavior, but it will not be active unless the node to avoid is within a configurable spatial envelope. The central IvP algorithm (the "captain') will then continuously calculate and publish an objective compromise, which will be passed on to the MVC via the MOOSDB and the interface process (the "Helmsman").

The *Nested Autonomy* paradigm in general allows the mode transitions to be entirely arbitrary, which makes it inherently suited to sensor-adaptive mission execution. Thus for example, an underwater vehicle operating in a *Deploy* mode such as a hexagonal loiter will use its onboard sensor processing to *Detect* and subsequently *Classify* an episodic event to which the node must respond. Once the processing is confident in assessing the desired nature of the event, it will simply change a MOOS variable which will trigger a mode transition in the Helm to a *Prosecute* mode, which will activate a set of behaviors that allows the vehicle to map and track the event.

Mode transitions may alternatively be triggered by a simple command from the operators, received via the communication infrastructure. Also, depending on the configuration, transitions may be initiated by an *Event Report* issued by a collaborating fixed or mobile node or the operators. The fact that mode transitions can be initiated through various channels is a key feature ensuring robustness. Thus, for example, a node which has not itself been able to detect an event can be alerted through one of the other channels and consequently participate fully in the event prosecution.

An example autonomy mode hierarchy for vehicles in a network deployed for capturing episodic oceanographic events is shown in Fig. 9. During a mission a vehicle will always reside in one of the modes at the end of a branch, and it will as a fundamental principle remain in that mode until it is commanded, internally or externally, to transition to another mode. Each mode defines a set of behaviors, most of which are generally available off-the-shelf. A typical behavior set is shown in the table in Figure 9.

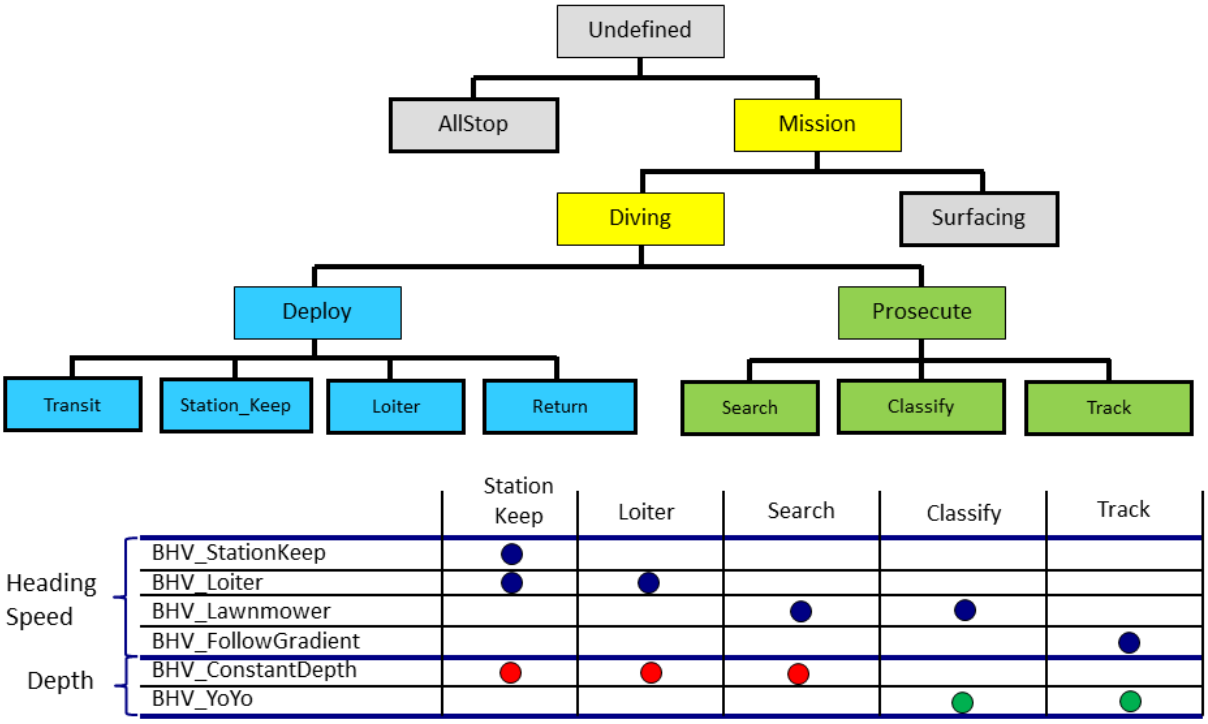


**Figure. 9.** Autonomy Mode hierarchy for autonomous detection, classification and tracking of an episodic oceanographic event such a coastal front. Each mode has a predetermined set of behaviors, defined in the table.

The perpetual mode/behavior architecture provides an extremely effective basis for executing field missions. Thus, except for configuration variables such as the operational area and initial deploy location, the autonomy software in general does not require modifications before each individual launch, and even the sensing mission itself may be modified after deployment because of the capability of issuing the vehicle a high level, simple command which switches the mode, modifies variables such as waypoint locations, or activates and de-activates onboard sensing resources. Thus, for example, a vehicle executing a sonar survey can with a single command be switched to a mission mapping the temperature and salinity over depth, as long as that particular survey mode and the associated behaviors (race track, depth-yoyo, etc.) have been defined in the autonomy configuration.

## 4. Acoustic Communication Infrastructure

The Nested Autonomy paradigm is inherently autonomy-centric, with the objective of making it robust to the severely constrained undersea communication environment with low bandwidth, high latency, and most importantly, severe intermittence imposed by the underwater acoustic environment. However, the operation of the observation network is still dependent on occasional communication to the vehicle in the form of commands changing the platform mode and configuration variables. Also, there is a need to send *Status*, *Contact* and *Track* reports to the

operators to allow them to make informed decisions regarding progress of the mission. Finally, for many ocean sensing missions, the environmental assessment performance can benefit significantly from collaborative platform behaviors because it has the potential of breaking the space-time ambiguity inherent to measurements made by individual moving platforms.

The MIT Nested Autonomy operational paradigm is using the Goby (Schneider and Schmidt, 2012) communication infrastructure and a highly flexible Dynamic Command and Control Language (DCCL) (Schneider and Schmidt, 2010, which together with a new Goby-Acomms communication marshalling, queuing and link layer (Schneider and Schmidt, 2013a,b) provides a highly portable and efficient, unified command and control architecture. This allows field deployments of undersea networks of modem-equipped AUVs with MOOS-IvP autonomy to become routine exercises (Schneider and Schmidt, 2010).

With each network node being directed by the MOOS-IvP platform autonomy system, the operational paradigm enables fully autonomous adaptation of the mobile network nodes to the environmental and tactical picture, collaborative target event tracking by multiple platforms, and safe and efficient operation in uncharted environments without the need for re-programming. Once deployed, the entire network is operated using only the DCCL messages for communication between nodes and human operators for changing mission objectives and platform states. The Goby-DCCL is interfaced to the MOOS-IvP platform autonomy by the process *pAcommsHandler*, as shown in Fig. 6, providing the following capabilities and properties to the autonomy system:

- Highly portable with most of the software being hardware-independent, with generic message handling all the way down to the physical modem driver.
- The DCCL encoding/decoding provides highly efficient data compression through a user-defined message composition with arbitrary value intervals and resolution.
- Dynamic queuing allows for high-priority messages to move to the head of the queue, with the priority of less time critical low-priority messages such as *Status* reports increasing with time. This ensures that the message queue not be saturated by high-priority, short time validity messages such as *Track* reports.
- User defined TDMA communication scheduling, either using a centralized polling scheme, a fixed slotted scheme, or a dynamic self-discovering slotted scheme.

## 5.0 On-Board, Real-Time Signal Processing

A key to the autonomous, adaptive sampling of chemical, biological, physical, or acoustic fields in the ocean is an efficient on-board implementation of a data analysis package that allows for real-time feedback to the platform control, allowing for the sensor-adaptive autonomous control of the platforms. MOOS-IvP provides a very effective infrastructure for achieving this due to its modular structure and well defined communication infrastructure. Thus, as illustrated in Fig. 6, separating the signal processing chain into a sequence of MOOS processes will allow each step in the processing to not only take advantage of the navigation information available in the MOOSDB, but also have the possibility of providing feedback to the Helm for optimizing the processing performance. This real-time, closed-loop feedback is the key enabler of environmentally *adaptive* sampling by making processed event data immediately available to the

autonomous control. Also, it allows the data processing to take advantage of information arriving from other network nodes and published in the MOOSDB, enabling more effective *collaborative* sampling when the communication environment allows.

## 6. Application Examples

In a collaborative effort between the NATO Undersea Research Centre (NURC), MIT, Woods Hole Oceanographic Institution (WHOI), and the Naval Undersea Warfare Center (NUWC), a series of experiments were carried out between 2008 and 2010, with the primary objectives being the demonstration of the performance of a network of underwater vehicles as receiver platforms for multistatic active sonar tracking, and their communication and control networking. In these experiments, up to seven Autonomous Underwater Vehicles were deployed, six of which were equipped with towed hydrophone arrays and operating in a common underwater acoustic communication network (Schneider and Schmidt, 2010). These experiments provided a unique opportunity for testing and demonstrated the performance of the Nested Autonomy control paradigm under realistic underwater communication constraints. The experiments were designed, in addition to the multistatic acoustic data collection, to allow the demonstration of fully autonomous oceanographic mapping and adaptive autonomous behaviors for optimal acoustic sensing and communication. They also provided a comprehensive testbed for the MOOS-IvP platform autonomy in general.

### 6.1 Unified Command, Communication and Control Infrastructure

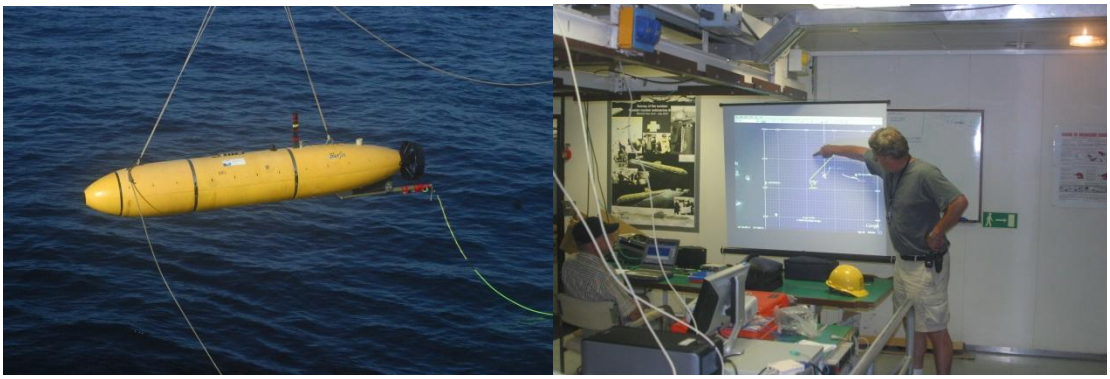

**Figure 10.** GLINT'08 Experiment, Pianosa, Italy, July-Aug. 2008. Left frame shows the Unicorn BF21 AUV with towed DURIP array (out of photo) being deployed from the NRV Alliance. Right frame shows the command and control center on the NRV Alliance with situational display.

The GLINT'08,'09, and '10 experiments were carried out as part of a Joint Research Project (JRP) on undersea sensing network technology (NURC project 4G4), involving NURC, MIT, WHOI, NUWC and several Italian organizations. The experiments had several scientific objectives, relating both to the sensing concepts, communication networking, and distributed, autonomous control.

The principal objective was to demonstrate the commmunication, command and control of a hybrid platform suite, using a common communication infrastructure based on the WHOI Micromodem, and a common autonomy system for operating all mobile and fixed assets, based on the 'Payload Autonomy' paradigm and the MOOS-IvP behavior-based autonomy software suite. The architecture had previously been intergrated and demonstrated on the SCOUT kayaks, the Bluefin BF21 AUVs (Figure 10), and several land robots at MIT. In preparation for and during GLINT'08, it was succesfully integrated into the NURC OEX AUV and the NUWC IVER-2 AUVs, both deployed in the experiment towing hydrophone arrays for multistatic acoustics. In addition, the architecture was partially integrated into the NUWC FOLAGA environmental sampler and two bottom moorings equipped with micromodems for undersea networking. The hybrid network with these assets is shown schematically in Figure 11.

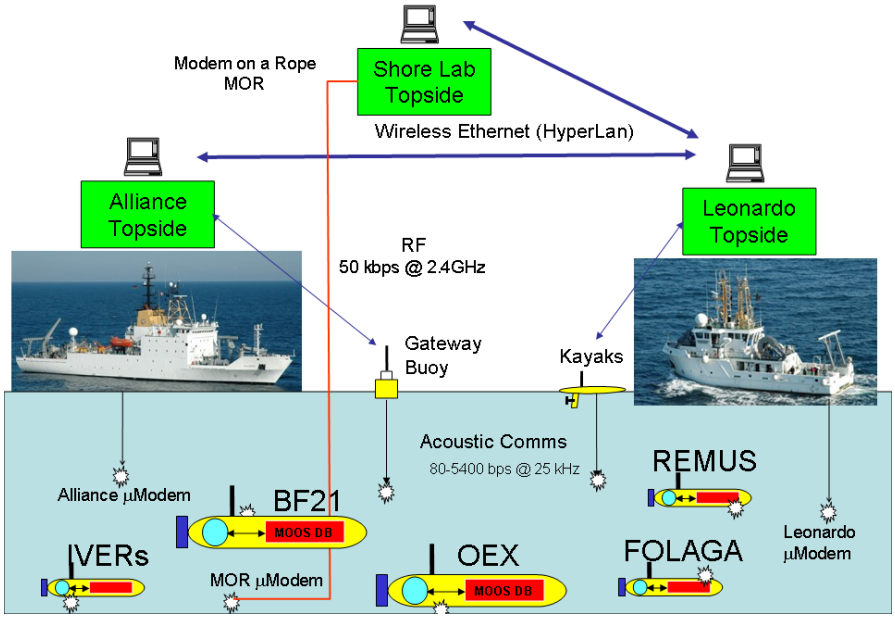


**Figure 11.** GLINT'08 hybrid vehicle and communication networking.

The principal scientific objective of GLINT'08 was to collect a comprehensive multi-static active dataset using three AUVs with towed hydrophone arrays, which will support the

development of robust multi-static active processing approaches suited for operation in the limited computational environment of AUVs. The three vehicles were the NURC OEX with the 48-element SLITA array, the MIT Unicorn BF21 with the 32-element DURIP array, and the NUWC IVER-2 vehicle towing a 16-element hydrophone array. The two large vehicles - the OEX and Unicorn - had fully integrated MOOS-IvP autonomy systems early in the experiment and were routinely used in coordinated data collection missions. On the last day of the experiment, all three array-towing vehicles were operated together. Also, the MOOS-IvP-DCCL communication infrastructure (Schneider and Schmidt. 2010) allowed several demonstrations of fully autonomous obstacle and collision avoidance to be performed by Unicorn and OEX, as illustrated in Fig. 12, which shows the topside real-time situational display, which graphically displays all status and contact information transmitted from the vehicles via the undersea communication network.

A major accomplishment in GLINT'08 was the development of an enhanced report and command structure which allows for dynamic, optimally compressed, encoding and decoding of messages (Schneider and Schmidt, 2010). This new Dynamic Compact Control Language (DCCL) communication handler was implemented in MOOS-IvP and demonstrated for real-time interleaved transmission of regular low-bandwidth FSK messages with high-rate PSK coded messages, for up to 2kbyte messages at 5.4kb/s, allowing for real-time transmission of CTD measurements and array signal processing products such as Beam-Time Records (BTRs) for real-time display on the topside situational display. The real-time topside display of BTR data from an AUV had not previously been achieved in the field. Acoustic communication messages from Unicorn and the other AUVs were assimilated with a heterogeneous mixture of other data sources (AIS, ship's NMEA, etc.) to give a unified situational display available to both the science crew and the ship's captain, as illustrated in the right frame of Figure 10 and the left frame of Figure 12. The left frame of Figure 12 shows an example of the usefulness of the situational display in a case of a run-away of one of the NUWC IVER-2 AUVs. The last reported navigation for the vehicle was extrapolated in the topside command center to determine a possible grounding site on the island of Pianosa. The workboat was subsequently sent to the predicted site at the northern tip, and the vehicle was recovered from the rocks within 10 m of the predicted location.


**Figure 12.** Real-time topside situational display in GLINT'08 command center on-board the NRV Alliance. The left frame shows extrapolation of navigation data for a runaway IVER-2 vehicle. The right frame shows the topside rendering of a Unicorn performing its obstacle avoidence and collision avoidance behaviors, with the WHOI Gateway buoy and the OEX AUV, respectively.

## 6.2 Adaptive Thermocline & Acousticline Tracking

One of the primary applications of this Nested Autonomy system is the autonomous and adaptive detection and tracking of oceanographic features with AUVs. To this end, algorithms for autonomous and adaptive thermocline tracking have been developed and extensively tested in field experiments, demonstrating the feedback loop between AUV sensor measurements and adaptive motion using the Nested Autonomy system.

To implement adaptive thermocline tracking on-board AUVs, a MOOS application named pEnvtGrad was written to interface thermocline detection algorithms with the MOOS and IvP Helm autonomy system. pEnvtGrad's final output simply consists of the upper and lower depth bounds of the thermocline region, as well as the depth at which the thermocline's temperature gradient ($|\Delta T/\Delta z|$) is largest. The upper and lower bounds of the thermocline are then used by an IvP Helm behavior (BHV_ToggleDepth) to bound the vertical motion of the AUV, producing a depth-adaptive yo-yo pattern in depth and effectively tracking the thermocline depth (see Fig. 5). In fact, pEnvtGrad also allows for similarly tracking the acousticline and pycnocline with the same algorithms, where sound speed and density values are based on temperature and salinity measurements from the AUV's on-board CTD. The details of the thermocline detection algorithms and pEnvtGrad are given in (Petillo, Balasuriya, & Schmidt, 2010).

Adaptive thermocline and acousticline tracking were demonstrated during the GLINT '09, Champlain '09, and GLINT '10 field trials, which are described below. The GLINT '10 experiment in particular used adaptive thermocline tracking missions in the broader context of collecting a synoptic multi-AUV data set displaying evidence of internal waves.

### *6.2.1 Acousticline Tracking (GLINT'09)*

**Figure 13.** The NURC OEX AUV during GLINT '09. This AUV uses acoustics to communicate with the ship while underwater and gets position updates via GPS when surfacing. Used with permission from(Petillo, Balasuriya, & Schmidt, 2010).

The GLINT ’09 experiment was a collaborative effort between MIT and the NATO Undersea Research Centre (NURC, based in La Spezia, Italy) that took place in the Tyrrhenian Sea near Porto Santo Stefano, Italy. Adaptive acousticline tracking missions took place on 13-14 July, 2009, using the NURC OEX AUV (Figure 13) running MOOS and IvP Helm autonomy. The AUV was deployed from the NRV Alliance, where the topside AUV operators monitored the AUV’s status via acoustic communication systems.

In preparation for at-sea testing, pEnvtGrad underwent development and testing in a simulation environment constructed from CTD data collected by the AUV in the same region earlier in the cruise. In developing pEnvtGrad, the acousticline was defined as the depth range over which the sound speed changes most rapidly per unit depth. For the associated in-water acousticline tracking missions that took place, the AUV was commanded into a north-south 1 km x 200 m racetrack pattern and performed the acousticline tracking as an adaptive-depth yo-yo pattern determined and autonomously updated by pEnvtGrad.

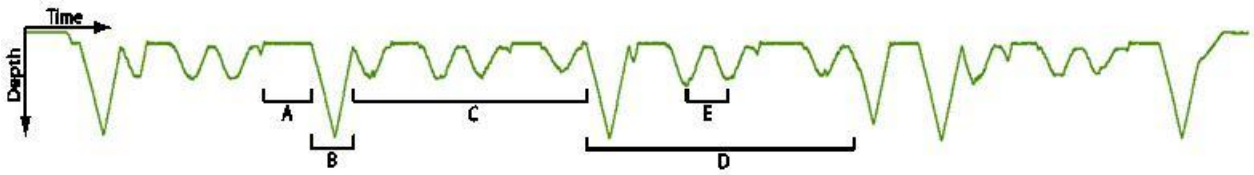


**Figure 14.** Depth history of the OEX AUV during an adaptive acousticline tracking mission. (A) is the default shallow turning and transiting depth (7m). (B) is the initial yoyo (7-70 meters) performed by the AUV to ensure sampling of the entire water column down to the vehicle's maximum dive depth. (C) is the adapted yo-yo tracking the acousticline between 9 and 28 meters depth. (D) is a 30-minute tracking

period after which the AUV re-initializes the yo-yo through the full water column to account for acousticline depth variation over space and time. (E) is the 400-meter period (length) of a single yo-yo. Used with permission from (Petillo, Balasuriya, & Schmidt, 2010).

The actual depth history of the OEX AUV over its ~2-hour acousticline tracking mission is shown in Figure 14. The initial yo-yo is apparent as the deep dive from 7 to 70 m (B), which is followed by the adaptive acousticline tracking between 9 and 28 m depth (C). The vertical resolution of the acousticline tracking is based on sound speed values averaged over depth bins to smooth out any higher frequency variations in sound speed. In this case the depth bins were chosen to be 1 m deep (given a water depth of about 105 m). As the AUV collected more sound speed measurements, these got averaged into the acousticline depth determination algorithms to update the acousticline bounds autonomously and adaptively. To avoid smoothing out all sound speed variations over time, a 30-minute periodic reset was implemented to essentially restart the algorithm with a new initial yo-yo (D).

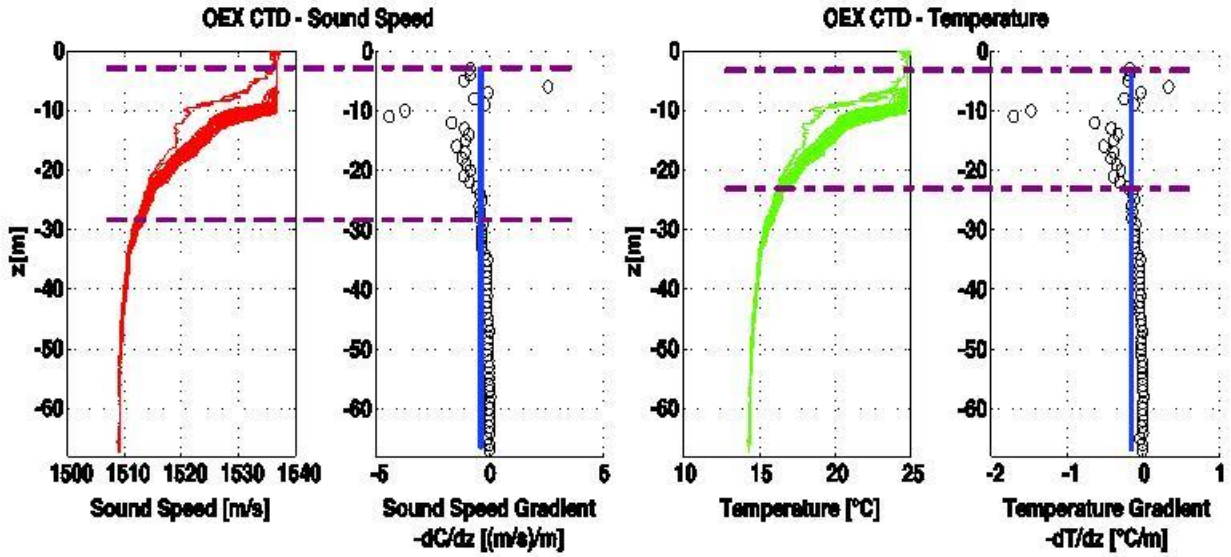


**Figure 15.** The leftmost plot of each pair gives the sound speed-depth (left) and temperature-depth (right) profile, respectively, over the entire mission (multiple dives). The rightmost plot of each pair shows the vertical sound speed (left) and temperature (right) gradients averaged over 1-meter depth bins. The solid vertical blue lines (on the gradient plots) represent the threshold values (average gradient over all sampled depths). A gradient greater in magnitude than the threshold magnitude is determined to be within the depth range of the acousticline or thermocline, respectively. The acousticline and thermocline regions are bounded by the dashed lines shown. Used with permission from (Petillo, Balasuriya, & Schmidt, 2010).

The post-processed vertical sound speed and temperature profiles from the full 2+ hours of data collected during the acousticline tracking mission are plotted in Figure 15. When calculating the sound speed with the MacKenzie Sound Speed Equation (1981) (MacKenzie, 1981), the sound speed is dominated by temperature in shallow water (as it is here) and by pressure deep in the ocean. This results in similarities in the shapes of the temperature and sound speed profiles in Figure 15. A thresholding method was used to delineate the acousticline and thermocline depth range, where the threshold was defined as the average of the sound speed and temperature

gradients, respectively, over all depth bins. The threshold total average sound speed gradient from post-processing $(\Delta c/\Delta z)_{tot\_avg}$ was 0.427 (m/s)/m and the average acousticline depth range was calculated to be 3-28 m, where c is the sound speed through the water in m/s and z is the negative of depth in meters. Similarly, the threshold total average temperature gradient from post-processing $(\Delta T/\Delta z)_{tot\_avg}$ was 0.162 °C/m and the average thermocline depth range was calculated to be 3-23 m, where T is the temperature in °C.

The discrepancy between the minimum depth boundary from post-processing and that calculated on board the AUV during acousticline tracking (3 m versus 9 m, respectively) is due to the depth range over which the calculations are being bounded (3-70 m vs. 7-70 m, respectively), where the post-processed data additionally include measurements taken during the AUV deployment and surfacing for GPS that skew the upper acousticline depth shallower by slightly decreasing the threshold value.

### *6.2.2 Thermocline Tracking (Champlain'09)*

**Figure 16.** The NUWC `Hammerhead' Iver AUV used during Champlain '09. This AUV carries a complete environmental package in its nose and communicates with the ship via RF (on the surface) and acoustics (underwater). It also carries a GPS and Doppler Velocity Logger (DVL) for positioning. Used with permission from (Petillo, Balasuriya, & Schmidt, 2010).

The Champlain '09 experiment took place in Lake Champlain, VT, USA from 3-5 October, 2009. A combined group from MIT and the Naval Undersea Warfare Center (NUWC, based in Newport, RI, USA) deployed an Iver AUV (Figure 16) running MOOS and IvP Helm autonomy software into this freshwater lake to test adaptive thermocline tracking missions. Since the Iver is a human-portable AUV, it was deployed off the side of a small motorboat and communicated with the operators on the boat via a 25 kHz WHOI Towfish acoustic transducer & Micro-modem system. Lake Champlain was chosen due to its proximity to MIT and NUWC and for its deep center channel (>100 m), which helps it support a stratified thermal structure that allows a thermocline to develop over the warmer months.

Champlain '09 was the second field trial of pEnvtGrad, where it underwent further testing and improvement while conducting adaptive thermocline tracking missions. In the horizontal plane, the AUV was deployed into a northwest-southeast straight line transect 1 km long. In the

vertical, the AUV performed a depth-adaptive yo-yo pattern across the thermocline depth, which was determined autonomously by pEnvtGrad.

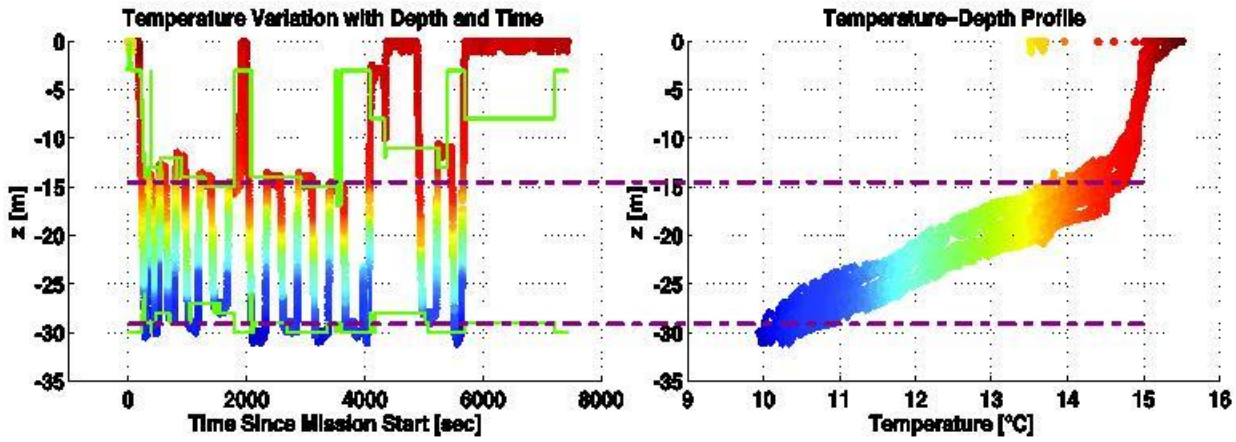


**Figure 17.** These data were taken from the real-time topside CTD display showing temperature variations over depth and time. The colors of the data on the left plot correspond to the temperature color coded by the right plot. The squared-off green lines across the plot on the left give the exact values of the thermocline boundaries as determined by pEnvtGrad throughout the mission. The dashed red lines approximate (by inspection) the average thermocline bounds as determined by pEnvtGrad. Used with permission from (Petillo, Balasuriya, & Schmidt, 2010).

The results of one of these thermocline tracking missions are shown in Figure 17, where the AUV was deployed for about 2 hours total and was deployed into a thermocline tracking mission for the first 1.5 hours. The left plot shows the actual depth of the Iver AUV (multi-color points), with the colors corresponding to the temperature at the given depth, time, and location along the horizontal transect (not shown). The associated temperature values are plotted in the temperature-depth profile on the right with the same color scale. On the left plot, the AUV performs an initial yo-yo from 3 to 30 m as the first dive, gathering temperature data, and then determines autonomously that the thermocline is between about 14 and 29 m depth (smaller amplitude undulations) and starts tracking the thermocline. The thermocline depth bounds actively calculated on the AUV by pEnvtGrad are plotted as the green lines on the left plot, which demonstrate the ability of the AUV to actively and autonomously adapt to changes in the thermocline depth boundaries (as small as 1 m) in real time. We chose 1 m depth bins because the water depth at the deployment location was on the order of 100 m, and the periodic reset was set at 30 minutes.

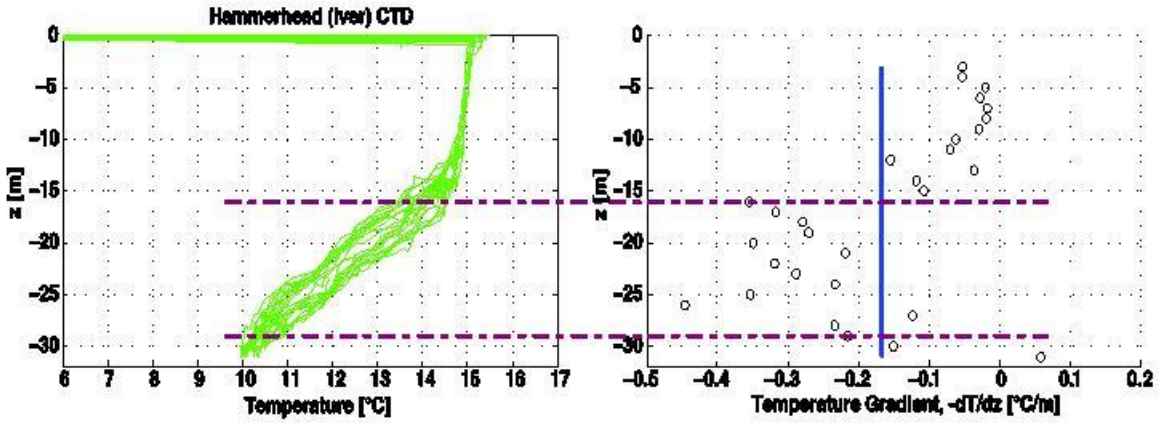


**Figure 18.** The plot on the left gives the temperature-depth profile over the entire mission (multiple dives). The plot on the right shows the vertical temperature gradients averaged over 1-meter depth bins. The solid vertical blue line (right) represents the threshold value (average gradient over all sampled depths). A gradient greater in magnitude than this average value's magnitude is determined to be within the depth range of the thermocline, the region bounded by the dashed lines. Used with permission from (Petillo, Balasuriya, & Schmidt, 2010).

The post-processed temperature data from the entire mission in Figure 17 is shown in Figure 18. The average thermocline depth range was calculated as about 16 to 29 m (dashed lines, Fig. 18) in post-processing, with the total average temperature gradient $(\Delta T/\Delta z)_{tot\_avg}$ of 0.168 °C/m set as the threshold value for bounding the thermocline range (solid vertical line, Fig. 18). When comparing the thermocline ranges determined by inspection of the AUV's actions in real time versus those calculated in post-processing (dashed lines, Figures 17 & 18, respectively), it is apparent that they are very similar (within a couple of meters), verifying the effectiveness of the real time calculations and adaptation.

In this experiment, the muddy lake bottom at an imprecisely known depth posed a risk to the recovery of the AUV, thus we could not let it dive deeper than about 35 m. This directly bounded the range of depths over which we could collect temperature data, which affected the threshold value used to bound the thermocline. Thus, it is likely that we did not capture the full range of the thermocline during the mission. However, since the thermocline range was determined by pEnvtGrad to extend down to 30 m in the real-time data (for safety the maximum thermocline depth was bounded at 30 m from the initial yo-yo settings), this demonstrates the ability of the AUV to detect the majority of the sampled thermocline range with pEnvtGrad algorithms even in cases where data are unavailable over part of water column.

*6.2.3 Thermocline Tracking for Internal Wave Detection (GLINT'10)*


**Figure 19.** The region of the Tyrrhenian Sea bounded by the western coast of Italy and the islands of the Tuscan Archipelago. The Tuscan Archipelago basin is outlined by the dashed line. The GLINT `10 AUV operation region is delineated by the box. The numbering shows the five inlets of the basin. Used with permission from (Petillo & Schmidt, 2014).

On 13 August, 2010, MIT and NURC conducted the Internal Wave Detection Experiment (a single-day experiment in the larger GLINT `10 experiment) in the northern coastal basin of the Tyrrhenian Sea bordered by the Tuscan Archipelago and the western coast of Italy (see Fig. 16). This experiment aimed to use Nested Autonomy and multiple AUVs to detect the presence of internal waves (or lack thereof) in this region of the Tyrrhenian Sea.

This experiment took a novel approach to internal wave detection by tasking two collaborating AUVs to autonomously adapt their motion in relation to each other and to their dynamic environment, resulting in greater efficiency of sampling given a restrictive mission duration and in collection of fully synoptic data sets capturing internal waves.

The Internal Wave Detection Experiment involved two AUVs running the MOOS autonomy system guided by the IvP Helm. These AUVs used acoustic communication during the experiment to send and receive real-time data and status updates, which they used to autonomously coordinate their motions in the horizontal plane through a track-and-trail behavior, as seen in the topside display in Fig. 20. In the vertical axis, the Unicorn AUV autonomously adapted to changes in the environment using the adaptive thermocline tracking behavior while the Harpo AUV (which would have also adapted, if the thermocline depth allowed for more reliable acoustic communication) swam just below the thermocline. A thermistor chain was also deployed for the duration of the experiment.

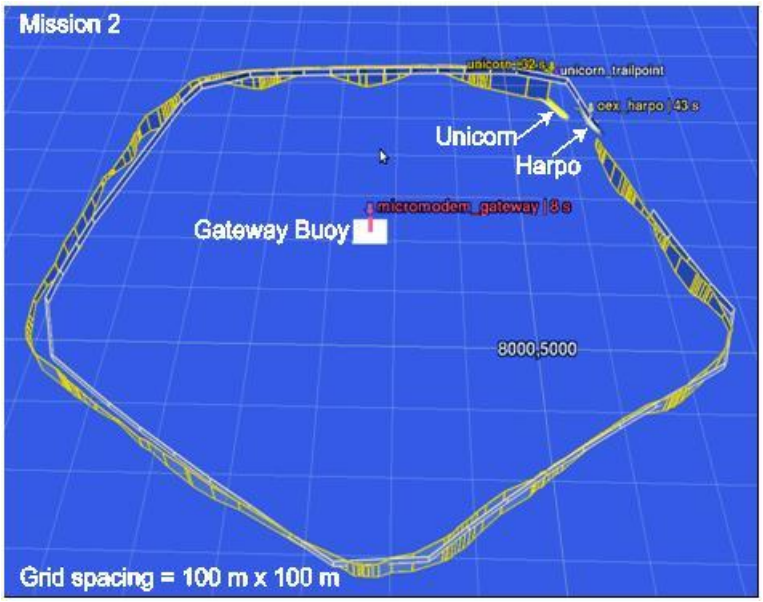


**Figure 20.** Mission 2 loiter pattern around the gateway buoy, as seen from above, at an angle to the horizontal. Harpo performs a horizontal loiter pattern at constant depth (12 m) just below the thermocline. Unicorn trails directly behind Harpo while performing an adaptive yo-yo pattern through the thermocline depth range. Vertical bars along the loiter indicate the AUVs' depths (yellow is Unicorn's track, white is Harpo's track), and their current positions are shown by the arrows. Used with permission from (Petillo & Schmidt, 2014).

In examining the resulting AUV and thermistor data sets from this experiment, there is strong evidence of internal wave propagation along the thermocline near the buoyancy frequency of the thermocline interface ($N_{max}$ = 0.05747 rad/s). Internal waves with nearly identical and lower frequencies were seen in the Unicorn, Harpo, and thermistor data collected near the thermocline depth. The 12 m depth AUV and 11 m depth thermistor results suggest the presence of buoyancy-supported internal waves along the thermocline (about 11 m depth) in the AUV operation region throughout the day on 13 August, 2010. This conclusion may also be extrapolated to say that internal waves are likely detectable along the thermocline throughout the rest of the Tuscan Archipelago basin during the summer, when the thermocline is fairly well defined. Given the lack of previous literature regarding internal waves in the Tuscan Archipelago basin, this finding is rather significant to the scientific groups that conduct acoustic (and other) experiments in this region. See (Petillo & Schmidt, 2014) for more detailed results and analysis from the Internal Wave Detection Experiment.

Overall, this experiment was novel in its use of multiple AUVs collaborating autonomously with each other and autonomously collecting environmentally-adaptive data sets for more synoptic spatiotemporal data coverage. Not only does this increase the efficiency of data collection (environmentally-adaptive autonomy behaviors allow us to collect the exact data set we need without a human in the loop), but it gives us the ability to collect the specific data set a scientist

is interested in by using AUVs running autonomy. The use of intelligent acoustic communication networking also allows the AUV operators and scientists to monitor (from the topside on a ship or shore) the data collected in near real time. These abilities are invaluable when ship time for data collection is so expensive, and we hope that such improvements in AUV autonomy, adaptive environmental sampling techniques, and acoustic communications will allow us to further reduce necessary ship time for scientists and engineers to collect the specific data sets they need in the future.

### 6.3. Bistatic Target Tracking (GLINT'10)

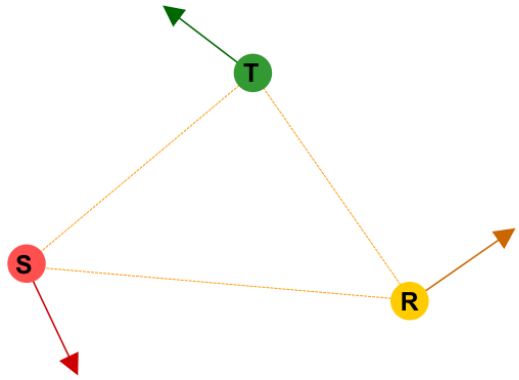


**Figure 21.** Two-dimensional bistatic geometry involving source (S), target (T), and receiver (R). The directional arrows indicate the velocities of the corresponding bistatic assets.

As part of the GLINT experiment program and associated research, the Nested Autonomy Paradigm was extended to the bistatic tracking of underwater targets. The concept of this application can be illustrated by the two-dimensional bistatic geometry in Figure 21. The passive acoustic receiver (denoted as R), constructed as a hydrophone array, is towed by an AUV in this application. The active acoustic source (denoted as S) is deployed to transmit known sonar pulse signals at time $t_k$, where $k = 1, \ldots N$ denotes the sonar ping number. The sonar pulse signals reach the receiver as two distinct dominant signals – the direct blast is the signal traveling straight from the source to receiver, and the indirect blast is the signal traveling from the source to receiver via acoustic scattering at the target (denoted as T). These signals are then recorded as hydrophone array data on the receiver. By processing the data, the target state – consisting of the Cartesian position and velocity – can be accurately estimated.

#### *6.3.1 Integrated Perception, Modeling, and Control*

A new *Integrated Perception, Modeling, and Control Paradigm*, as shown in Figure 22, has been introduced for the AUV/receiver to solve the bistatic tracking problem (Lum & Schmidt, 2011; Lum, 2012). The *Automated Perception*, on the feedback path, is used to process the

hydrophone array data from the receiver, and provide the target state estimate. This perception is performed using sonar signal processing and target tracking algorithms. The estimate is the perceptive feedback in the closed-loop control system for driving both the *Perception-Driven Control* and *Unified Model*. The *Perception-Driven Control* then deliberates the perceptive feedback against the mission-level objectives to make unsupervised decisions on the speed and heading for the *AUV Motion* in the feed-forward path. No depth decision is considered here since Figure 21 is dealing with two-dimensional geometry. By controlling the *AUV Motion*, the vehicular path is adjusted adaptively. A new *Bistatic Behavior* has been developed in the *Perception-Driven Control* to execute, in real-time, a new non-myopic and adaptive control for the vehicle. The predictive information and environmental rewards from the *Unified Model* are used to provide the IvP function for this new behavior. The *Unified Model* is amalgamated from both information theoretic and environmental acoustic models. These models are then used to predict the pertinent information and acoustic characteristics of the target state estimate for the particular bistatic geometry. The pertinent characteristics predicted for different future bistatic geometries, resulting from different discrete speed and heading decisions at the current target state estimate, are then encapsulated in the predictive rewards. In essence, the control formulation presents a new vehicular control that applies both information-theoretic and environmental-based controls concurrently.

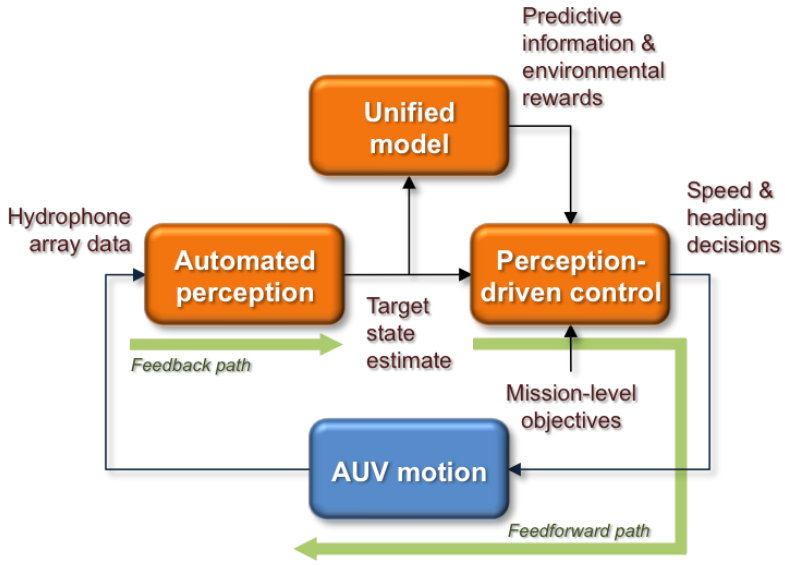


**Figure 22.** Integrated Perception, Modeling, and Control Paradigm for the AUV/receiver to solve the bistatic tracking problem.

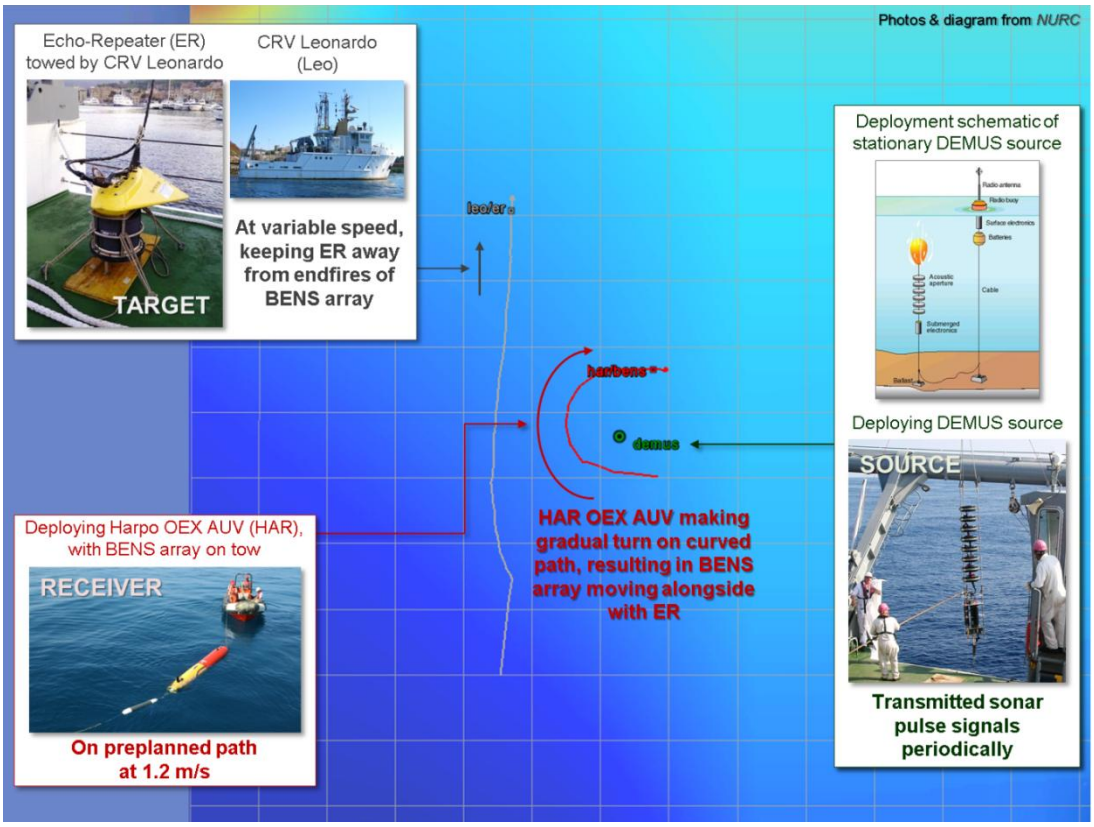


**Figure 23.** Ground truths of bistatic assets for a GLINT '10 experimental run with photos and schematic diagram. The DEMUS source is plotted in green, the Harpo OEX AUV towing BENS array is plotted in red, and the CRV Leonardo towing the Echo Repeater (ER) is plotted in gray. The historical Cartesian positions of bistatic assets are depicted, with their current speed and heading indicated by the length and direction of the arrow at their current positions. The AUV was commanded to move along a preplanned path at 1.2 m/s – heading west first, before making a gradual turn on the curved path, and then heading east. CRV Leonardo was cruising northward at variable speed, trying to keep the target away from the endfires of the receiver.

### *6.3.2 AUV on Preplanned Path*

To demonstrate the advantage of this new *Integrated Perception, Modeling, and Control Paradigm*, the bistatic tracking results of the underwater target are compared with the AUV operating with and without this new paradigm. We will first examine the tracking results without this paradigm. The data we use are from the GLINT '10 experimental run, conducted jointly between MIT and NURC, in the Tyrrhenian Sea off the coast of Italy. The ground truths of the bistatic assets utilized for this experimental run, together with their respective photos and schematic diagram, are depicted in Figure 23. The Deployable Experimental Multistatic Undersea Surveillance (DEMUS) source was deployed as stationary asset, and transmitting sonar pulse signals. The Echo-Repeater (ER) was used to simulate a target by retransmitting the recorded sonar pulse signals from the source. It was towed by the CRV Leonardo (Leo). The receiver was the BENS array, towed by the Ocean Explorer (OEX) AUV. The AUV was

commanded to move along a preplanned path at 1.2 m/s, for the entire run from ping $k$ = 1 to 235, without adopting the new paradigm. The AUV headed west first, before making a gradual turn on a curved path, and then headed east. The *Automated Perception* was used to process the hydrophone array data from the receiver and provided the target state estimate. However, this estimate was not used in the control. CRV Leonardo was cruising northward at variable speed, trying to keep the target away from the forward and aft endfires of the receiver array. This was done to ensure good tracking results on the target.

The bistatic tracking results from the *Automated Perception* for this experimental run at ping $k$ = 234 are shown in Figure 24. Both the confirmed and terminated tracks are clearly plotted, and the information pertaining to these tracks are depicted. For the confirmed track due to the ER, the information "t70:k = 176/rank = 2" implies that track #70 has been active for 176 pings since initiation and is ranked #2 in the active track priority. This track depicts the state estimated for the target over the past 176 pings. Track #122 is due to the ghost of the ER. This is caused by the starboard/port side ambiguity of the BENS array. However, this ghost is not well tracked because the constant maneuvering by the AUV, particularly during the gradual turn on the curved path, causes the track to violate the nearly constant velocity (NCV) target dynamic model assumed in the *Automated Perception*. Tracks #11 and #413 are due to the prominent fixed but unknown underwater objects that were persistently present since the start of the experimental run. With the target speed, good target tracking results are obtained for track #70.

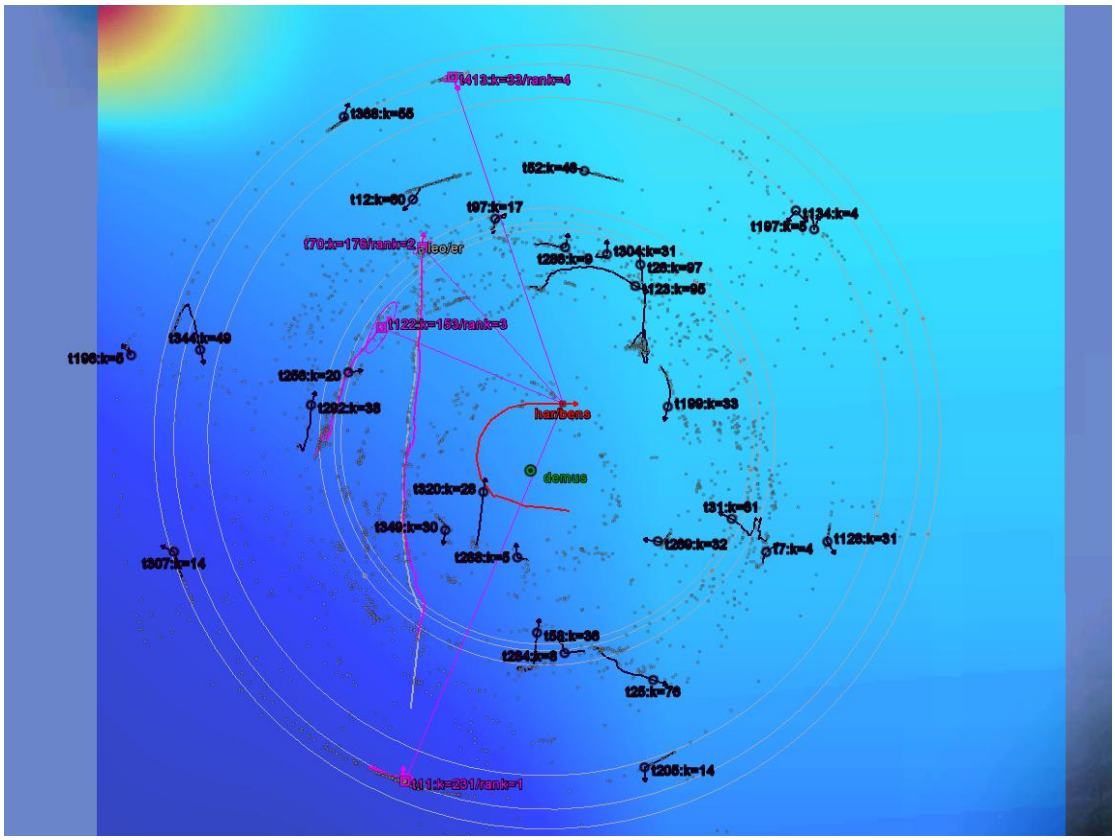


**Figure 24.** Bistatic tracking results from *Automated Perception* for the GLINT '10 experimental run at ping $k$ = 234. The ground truth of the DEMUS source is plotted in green, the Harpo OEX AUV towing the BENS array is plotted in red, and the CRV Leonardo towing the ER is plotted in gray. Confirmed tracks are plotted in magenta, terminated tracks are plotted in black, and information pertaining to these tracks is depicted. For confirmed tracks due to the ER, information "t70:k = 176/rank = 2" implies track #70 has been active for 176 pings since initiation and is ranked #2 in active track priority. This track depicts the state estimated for target over past 176 pings. Track #122 is due to a ghost of the ER (because of starboard/port side ambiguity of the BENS array). Tracks #11 and #413 are due to prominent fixed but unknown underwater objects.

### *6.3.3 AUV on Adaptive Path*

In the previous section, the bistatic tracking results were obtained with the AUV on a preplanned path. The AUV was not reacting to the target state estimate obtained from the *Automated Perception*. The target speed was adjusted to keep the target away from the endfires of the receiver. This was done to ensure good tracking results on the target. Operationally, this is not realistic since the target is never cooperative. In this section, we will implement the *Integrated Perception, Modeling, and Control Paradigm* on the AUV. The synthetic data, generated from a high-fidelity simulator, is used here with the same bistatic assets as the experimental data in Figure 23. The simulated tactical scenario is shown in Figure 25. For this scenario, the stationary DEMUS source was simulated to transmit sonar pulse signals. The ER, towed by the CRV Leonardo, was used to simulate a non-cooperative target cruising eastward at a fixed speed

of 2 m/s from ping $k$ = 1 to 650. The OEX AUV, towing the BENS array, was commanded to move along the fixed path initially. With the new paradigm implemented on the AUV, the target state estimate of the ER from the *Automated Perception* is now used to drive both the *Perception-Driven Control* and *Unified Model*.

The simulated results of the tactical scenario at different pings $k$ are obtained in Figure 26. The target state estimates of the confirmed track #27 due to ER from the *Automated Perception* were used to drive the *Perception-Driven Control* and *Unified Model*. The AUV was initially moving on a fixed path, but switched to an adaptive path upon tracking the entry of the ER. This adaptive path was planned with the *Bistatic Behavior* in the *Perception-Driven Control*, with the objective of maximizing the information and acoustic performance of the target state estimate. With the adaptive path taken by the AUV, good target tracking results are obtained for track #27.

From the results obtained in Figures 24 and 26, it is clear that the *Integrated Perception, Modeling, and Control Paradigm* allows the path of the AUV to be adaptively adjusted in reaction to the target state estimated from the tactical situation. The path has been planned with the objective of optimizing the target tracking performance. Such methodology can be easily extended for distributed nodes in an AUV network.

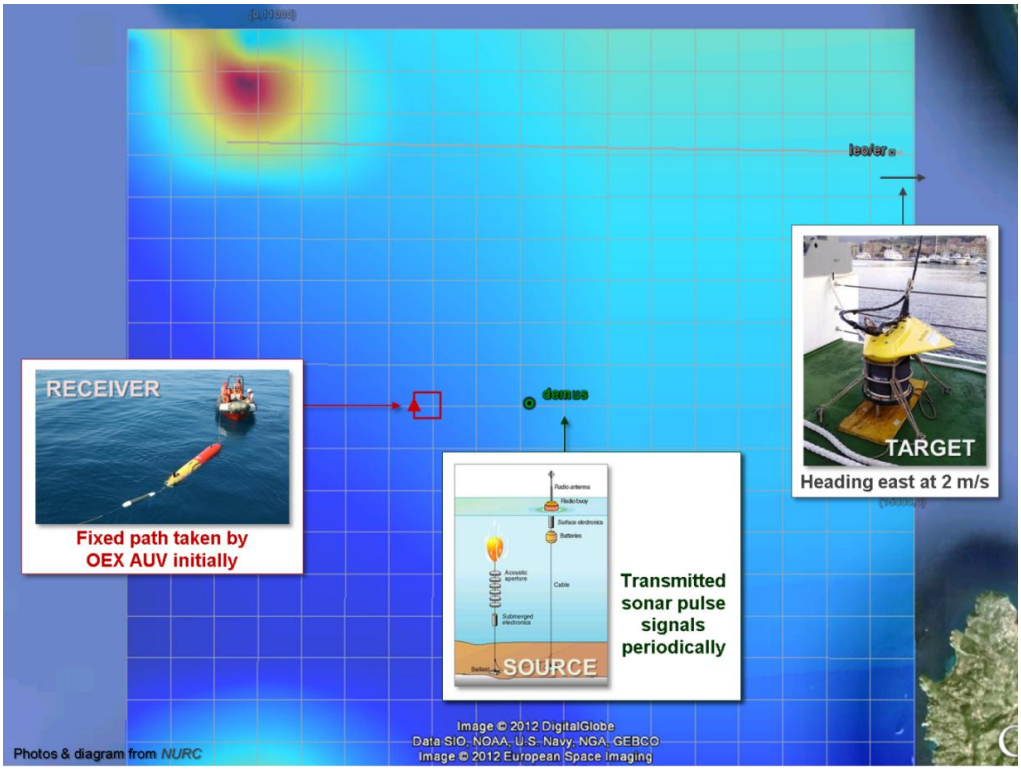


**Figure 25.** A simulated tactical scenario with the stationary DEMUS source plotted in green, the initial fixed path taken by the OEX AUV plotted in red, and the CRV Leonardo towing the ER plotted in gray. CRV Leonardo was simulated to head east at 2 m/s.

(a) $k$ = 75

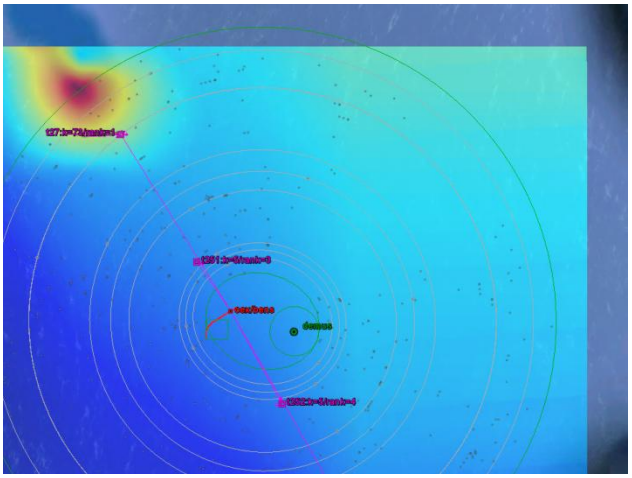

(b) $k$ = 275

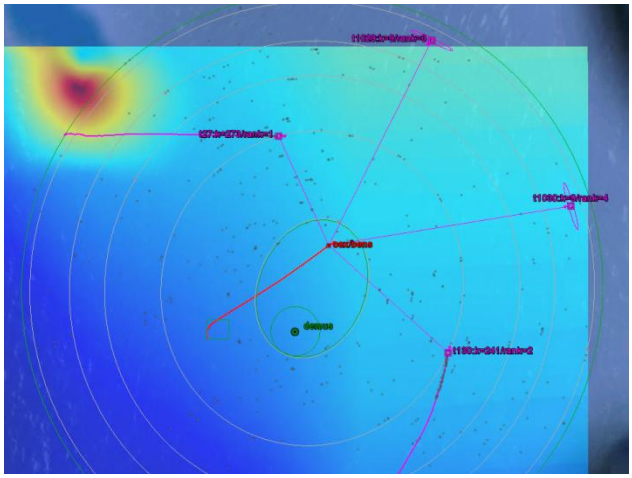

(c) $k$ = 385

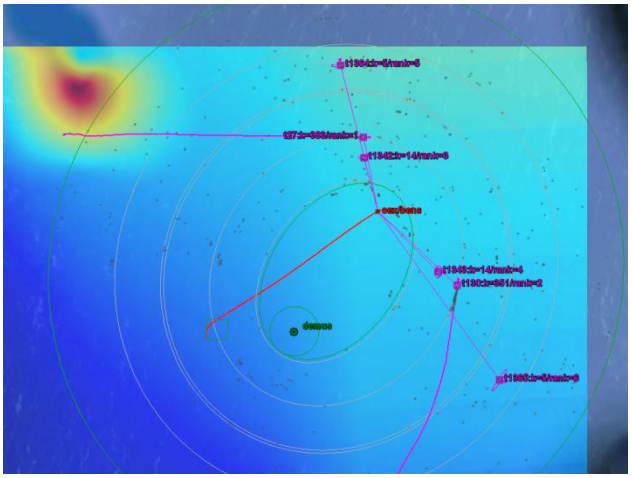

(d) $k$ = 475

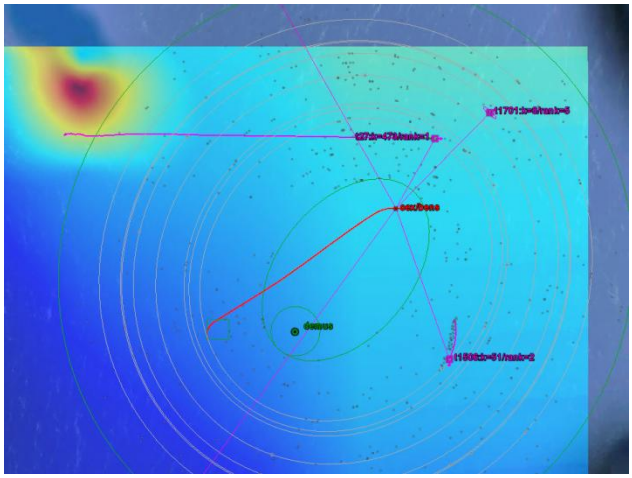

*(e) $k$ = 575*

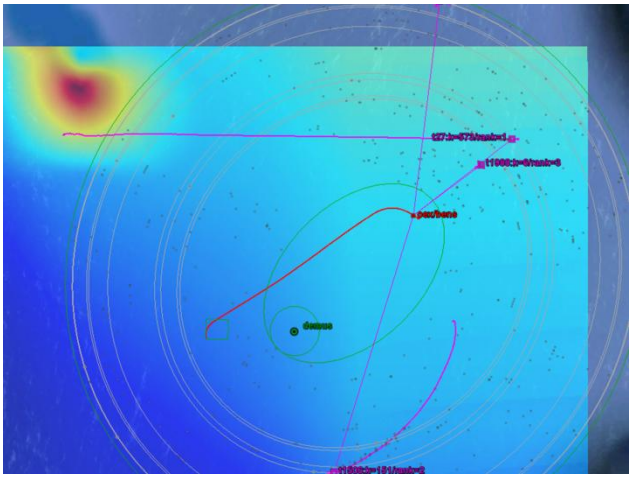

**Figure 26.** Simulated results of a tactical scenario at different pings $k$ with *Bistatic Behavior* applied on the OEX AUV and driven by target state estimates of the confirmed track #27 from the ER. The stationary DEMUS source is plotted in green. The OEX AUV towing the BENS array is plotted in red. The OEX AUV was initially moving on a fixed path, but switched to an adaptive path upon tracking the entry of the ER. The moving ER, towed by the CRV Leonardo, is plotted in gray (not visible) and was heading east. Confirmed tracks are plotted in magenta.

## 7. Conclusion

Being dependent on acoustic communication with a channel capacity many orders of magnitude smaller than the air- and land-based equivalents, the operation of distributed ocean sensing networks require a much higher level of autonomous, distributed data processing and control than land- and air-based equivalents. The *Nested Autonomy* paradigm and its underlying principle of *Integrated Sensing, Modeling and Control* described here are inherently suited for the layered communication infrastructure provided by the low-bandwidth underwater acoustic communication and the intermittent RF connectivity. Implemented using the open-source MOOS-IvP behavior-based, autonomous command and control architecture, Nested Autonomy allows each platform to autonomously detect, classify, localize and track (DCLT) an episodic ocean event without depending on operator command and control. The prosecution of a particular event may be initiated by the operators through an acoustically transmitted compact command message, cued by other sensing systems, such as satellite remote sensing, for example, or fully autonomously by an on-board detection algorithm, but the fundamental principle of the paradigm is that each network node shall be capable of completing its missions objectives, irrespective of communication connectivity. The inferred properties of the event are reported back to the operators by transmitting a compact *Event Report*, using a dedicated command and control language. Collaborative processing and control may be exploited when the communication channel allows, e.g. for collaborative tracking of extended features such as plumes and fronts. The nested command and control paradigm has here been demonstrated for the fully autonomous, adaptive tracking of the space- and time-varying coastal thermocline and acousticline, using relatively simple onboard signal processing, but the highly modular MOOS-IvP architecture allows the event characterization and tracking algorithms to be exchanged with customized and advanced processing software without altering the operational functionality of the autonomy system.

## Acknowledgements

The development of the fundamentals of the Nested Autonomy concept, and the MOOS autonomy system were performed at MIT with support from the Office of Naval Research Code 32 under the GOATS program (Thomas B. Curtin, Jeffrey Simmen, Randy Jacobson and Tom Swean, Program Managers) and the IvP extension was performed at MIT and NUWC under support from Dr. Don Wagner and Dr. Behzad Kamgar-Parsi from ONR Code 31. The operational paradigm and the associated MOOS-IvP configuration have subsequently been further developed and applied in several major field experiments under the ONR GOATS (Thomas B. Curtin, Ellen Livingston, and Bob Headrick, Program Managers), SWAMSI (Bob Headrick , Program Manager), and PLUSNet Undersea Persistent Surveillance (Thomas B. Curtin, Program Manager) programs, and most recently the DARPA DSOP Program (Andy Coon, Program Manager). The specific application of the concept to the adaptive tracking of the thermocline was performed under the ONR Adaptive

Sampling and Prediction (ASAP) MURI (Thomas B. Curtin, Program Manager) and supported by the U.S. Department of Defense (DoD), U.S. Air Force Office of Scientific Research, and National Defense Science and Engineering Graduate (NDSEG) Fellowship 32 CFR 168a.

The first field demonstration of MOOS and the early version of the Nested Autonomy control paradigm were performed in the BP02 experiment in La Spezia, Italy, carried out jointly with the NATO Undersea Research Centre (NURC), who supplied engineering and operational support. The GLINT'08-'10 experiments were also carried out in collaboration with NURC, and the authors appreciate the assistance from NURC for their exceptional engineering and operational support, and the use of their OEX AUV for the thermocline mapping and multistatic acoustic experiments described here. The collaboration with Naval Undersea Warfare Center (Michael Incze, Scott Sideleau, and Dr. Don Eickstedt) Code 25 & the ONR Lightweight NSW UUV program in the Lake Champlain'09 experiment is highly appreciated.

## References

Benjamin, M. (2002). Multi-Objective Autonomous Vehicle Navigation in the Presence of Cooperative and Adversarial Moving Contacts. *In Proceedings of OCEANS 2002.* Biloxi, MI.

Benjamin, M., Battle, D., Eickstedt, D., Schmidt, H., & Balasuriya, A. (2007). Autonomous control of an autonomous underwater vehicle towing a vector sensor array. *IEEE Proc. 2007 Int. Conf. Robot. Autom.*, (pp. 4562-4569). Rome, Italy.

Benjamin, M., Schmidt, H., Newman, P., & Leonard, J. (2010). Nested autonomy for unmanned marine vehicles with MOOS-IvP. *Journal of Field Robotics , 27* (6), 834-875.

Lum, R. (2012). *Integrated perception, modeling, and control paradigm for bistatic sonar tracking by autonomous underwater vehicles.* Ph.D. Thesis, Massachusetts Institute of Technology, Cambridge, MA.

Lum, R., & Schmidt, H. (Jun. 2011). Exploiting adaptive processing and mobility for multistatic tracking by AUV networks. *Proc. 4th Int. Conf. Underwater Acoustic Measurements: Technologies and Results*, (pp. 1487-1495). Kos, Greece.

MacKenzie, K. V. (1981). Nine-term equation for the sound speed in the oceans. *The Journal of the Acoustical Society of America , 70* (3), 807–812.

Petillo, S., & Schmidt, H. (Jan. 2014). Exploiting Adaptive and Collaborative AUV Autonomy for Detection and Characterization of Internal Waves. *IEEE Journal of Oceanic Engineering* , 39(1), 150-164.

Petillo, S., Balasuriya, A., & Schmidt, H. (2010). Autonomous Adaptive Environmental Assessment and Feature Tracking via Autonomous Underwater Vehicles. *Proceedings of IEEE OCEANS'10 Conference.* Sydney, Australia.

Schneider, T. and Schmidt, H. (2010), "Unified command and control for heterogeneous marine sensing networks." *Journal of Field Robotics*, 27(6), 876-889.

Schneider, T. and Schmidt, H. (2013a) "Model-based Adaptive Behavior Framework for Optimal Acoustic Communication and Sensing by Marine Robots", *IEEE J. Oceanic Eng.*, Vol. 38, No. 3, 522 – 533.

Schneider,T and Schmidt, H. (2013b) "A State Observation Technique for Highly Compressed

Source Coding of Autonomous Underwater Vehicle Position," *IEEE Journal of Oceanic Engineering*, Vol. 38, No. 4, 796-808.

Schneider, T. and Schmidt, H. (2012a), "Goby-Acomms version 2: extensible marshalling, queuing, and link layer interfacing for acoustic telemetry," in *Proceedings of the 9th IFAC Conference on Maneuvering and Control of Marine Craft*, Arenzano (GE), Italy, 2012.

Schneider, T. and Schmidt, H. (2012b), "Approaches to Improving Acoustic Communications on Autonomous Mobile Marine Platforms," in *Proceedings of the UComms 2012 Conference*, Sestri Levante (GE), Italy.